UNIVERSITY OF OKLAHOMA

GRADUATE COLLEGE

FRACTURING OPTIMIZATION BASED ON DYNAMIC CONDUCTIVITY

A THESIS

SUBMITTED TO THE GRADUATE FACULTY

in partial fulfillment of the requirements for the

Degree of

MASTER OF SCIENCE

By

PURACHET PATTAMASINGH
Norman, Oklahoma
2016

FRACTURING OPTIMIZATION BASED ON DYNAMIC CONDUCTIVITY

A THESIS APPROVED FOR THE
MEWBOURNE SCHOOL OF PETROLEUM AND GEOLOGICAL ENGINEERING

BY

_____
Dr. Rouzbeh G. Moghanloo, Chair

_____
Dr. Chandra Rai

_____
Dr. Deepak Devegowda

I would like to dedicate this thesis to my parents, Lanjakorn Pattamasingh and Kwanroen Jitjaroen for their support both financially and mentally. I also want to dedicate this thesis to my friends and colleagues who provided me with wonderful experiences and suggestions during my time in the USA.

Acknowledgements

I would like to thank to my advisor, Dr. Rouzbeh G. Moghanloo for his advice on this study. Without his guidance and ideas, this would not be sufficient research. I would also like to thank Dr. Rai and Dr. Deepak for their help with revisions and comments on this thesis. Furthermore, I would like to thank Mr. Ronnie Irani and RKI (Exploration and Production) company for providing me with reservoir description and PVT data.

Table of Contents

List of Tables

List of Figures

Abstract

This thesis presents a systematic approach to evaluate and optimize production performance of fractured wells in tight oil formations. Underperformed hydraulically fractured wells have been widely reported; poor design is often considered as the explanation; i.e. base line conductivity or Unified Fracture Design (UFD) is adopted without incorporating conductivity damaging parameters such as multiphase flow, non-Darcy flow, proppant embedment, fine migration and plugging, and proppant diagenesis. Therefore, we do not often observe the anticipated productivity in practice. This thesis is driven by the following hypothesis: "the predominant damaging parameters varies with fracture widths". Moreover, reducing the cost of fracturing while maintaining the same productivity for fractured wells has become one of the main challenges of the industry.

The unfavorable effects of proppant embedment, inappropriate proppant placement, gelling damage, fines migration and pore blockage, and cyclic stress on well productivity are investigated. A sensitivity study is performed using experimental design to evaluate significance of the damaging parameters for a range of fracture widths. In addition, net present value (NPV) and profitability ratio (PIR) are used for economic evaluation of three types of proppants: sand, ceramic, resin coated sand (RCS). Finally, optimization of fracture design is performed using PIR approach.

The results indicate that the damaging parameters can decrease cumulative production by 73 % in the examples studied here. The proppant embedment and proppant placement are dominant damaging mechanisms for fractures with small width. However, gelling damage and cyclic stress are the most sensitive parameters for fractures with large width.

Overall, RCS proppants demonstrate better performance, NPV, and PIR over ceramic and sand proppants for all range of proppant concentration in the studied examples. Using PIR approach, an optimal fracture half length of 400 ft is achieved for low average proppant concentration of 0.17 lb/ft^2 for RCS proppant. In addition, the PIR approach suggests an optimal fracturing scenario with 16% less initial cost compared to the NPV approach without significant reduction of the profit.

The outcome of this research will provide the field operators with remarkable knowledge on how to do a better fracturing design.

Chapter 1: Introduction

Last decade, unconventional reservoirs played an important role for supplying oil and gas. Technology development in drilling and completion such as horizontal drilling and hydraulic fracturing make these reservoirs economically viable to produce (Saldungaray and Palisch 2012). Specifically, multi-stage hydraulic fracturing allows a large volume of reservoir contact by creating a high conductivity pathway, which is crucial, especially for reservoirs with a nanodarcy permeability scale. Hence, hydraulic fracturing becomes standard practice for tight oil and gas, coal bed methane, and shale oil and gas formation development (Economides and Wang 2010).

Tight oil is a type of unconventional reservoir that refers to oil production from very low permeability sandstone, shale, or carbonate formations (EIA 2013). Development of tight oil is the center of attention because it is more economical than shale gas to produce. Unconventional reservoirs have different characteristics from conventional reservoirs, including nano-pore size, ultra-low permeability, overpressure, and large fraction of light component. Overpressure is one of the significant parameters that makes tight oil production economically successful, as the pressure gradient can be up to 0.8 psi/ft. From these characteristics, pore confinement and rock compaction contributes significant effects on rock properties and well productivity (Xiong et al. 2015).

The performance of hydraulic fracture relies on fracture conductivity and dimensionless fracture conductivity (C_{fD}) as shown in **Equation 1 and 2**. Fracture is considered to have infinite conductivity when C_{fD} is greater than 100

$$\text{Fracture conductivity} = k_f * w \quad (1)$$

$$C_{fD} = \frac{k_f * w}{k * x_f} \quad (2)$$

where k_f is the fracture permeability, w is width of fracture, x_f is half-length of fracture, and k is reservoir permeability. Economides, Valko, and co-workers as in (Romero et al. 2002) introduced the Unified Fracture Design (UFD) approach to optimize fractured well performance by indicating fracture geometry for a given proppant volume, reservoir and proppant permeability. The dimensionless proppant number is defined in **Equation 3** as

$$N_p = I_x^2 C_{fD} = \frac{4x_f k_f w}{k x_e^2} = \frac{4x_f k_f wh}{k x_e^2 h} = \frac{2k_f V_f}{k V_r} \quad (3)$$

Where I_x is penetration ratio, x_e is length of a square drainage area (well is in the center), V_f is volume of the propped fracture in the pay, and V_r is reservoir drainage volume. If the proppant number (N_p) is less than 0.1, the optimal C_{fD} value that maximizes dimensionless productivity index is 1.6. Optimal C_{fd} increases when N_p is larger than 0.1. Once Optimal dimensionless fracture conductivity C_{fDopt} is defined from **Equation 3**, the optimal fracture half-length (x_{fopt}) and width (w_{opt}) can be defined as **Equation 4 and 5** respectively:

$$x_{fopt} = \left(\frac{k_f V_f}{2 C_{fDopt} k h}\right)^{0.5} \quad (4)$$

$$w_{fopt} = \left(\frac{C_{fDopt} k V_f}{2 k_f h}\right)^{0.5} \quad (5)$$

However, there are some design flaws incorporated into the UFD approach. For example, selection of proppant size and type, damaging of proppant from gel residue and fracturing fluid leak off, and non-Darcy flow in high rate gas well are not considered (Economides and Wang 2010). To evaluate and optimize the well performance of tight oil reservoir precisely and accurately, Dynamic conductivity of fracture which incorporates conductivity damaging parameters such as gelling damage, proppant embedment, fine

migration and plugging, and etc. must be used instead of baseline conductivity. The objective of this research is to study effects of damaging mechanisms on well productivity of hydraulically fractured wells. The research is driven by the following hypothesis: "the predominant damaging parameters varies with the fracture widths". This thesis is structured as follows:

1. The factors that impact fracture geometry and conductivity are discussed. These factors include hydraulic fractures, proppant and fracturing fluid. These factors greatly dictate ultimate recovery of tight oil reservoir.
2. Conductivity damaging parameters are discussed and incorporated into both hydraulic fracturing and reservoir models to duplicate realistic fracture conductivity (Dynamics) for Niobrara tight oil reservoirs with proper rock and fluid properties.
3. Impacts of damaging parameters on well productivity are investigated which is structured as follows: 1) gelling damage, 2) proppant embedment, 3) proppant transport and placement, 4) cyclic stress, 5) fine migration and plugging and 6) Combination of damaging parameters. A sensitivity study of each damaging parameter on well performance for two different fracture widths are carried out. Subsequently, proppant selection can be determined based on net present value (NPV) and profitability ratio (PIR) by incorporating damaging parameters related to particular types of proppant. Finally, optimization of fracture half-length and average proppant concentration are examined for certain reservoir conditions.

1.1 Factors that Impact Well Productivity

In this section, I will provide overview of factors that influence well productivity of hydraulic fractured tight oil wells. Fracturing designs can be divided into many components. Fracture geometry is dictated by fracturing fluid properties, such as viscosity (leakoff coefficient), volume, and injection rate. Also, rock properties such as Young's Modulus can alter fracture growth. The geometry of fracture is one of the important criteria of fracturing design. For example, fracture growth into non O/G bearing zones is not only waste money, but it might create connection between aquifer/gas cap zones and the wellbore, which can deteriorate well performance (Yang et al. 2013). On the other hand, proppant is used to keep fractures open when confining stress is applied to the fracture, so propping agents create high conductivity pathways between the wellbore and reservoir rock. Moreover, proppant type can vary fracture conductivity due to many factors such as crushing resistance.

1.1.1 Hydraulic Fracture

Without stimulation techniques such as hydraulic fracturing, low and very low permeability reservoirs cannot be produced economically. Hydraulic fractures are created by pumping fluid downhole with pressure higher than rock tensile strength. The orientation of the fracture is perpendicular to minimum stress, so vertical fracture geometry is expected for moderate to deep wells. Hydraulic fracture can improve reservoir and wellbore contact. For example, simple planar bi-wing 200 ft. half fracture length with 50 ft. fracture height can increase reservoir contact by 350 to 10,000 times (Shah et al. 2010). However, fluid leak off from fracture face to neighboring areas with plane of weakness can create induced fracture, resulting in a complex fracture network

(Suarez-Rivera et al. 2013). Induced fractures are indicated by very small widths containing no proppant. As a result, induced fractures tends to close with increased net confining stress and lose conductivity by orders of magnitude. Hydraulic fracture models were originally developed by Perkins and Kern (1961) and Geertsma and de Klerk (1969), which were based on 2 dimension fractured systems as shown in **Figure** 1. Both models were developed with fixed fracture height assumption, and fracture shape is assumed to be elliptical. However, PKN assumption of elliptical shape is parallel to the cross section of fracture height, while the elliptical shape is perpendicular to the fracture opening for GDK models as shown in **Figure 1.** In addition, fracture geometry prediction is longer length and narrower width for PKN models, while fracture geometry that is predicted by GDK models to have shorter length and wider width. Both models are considered great improvement in hydraulic fracture modeling, but the limitation is the inability to forecast fracture height. Next, gridded finite element fracturing simulation is introduced to predict fracture geometry in three dimension due to advances in computer capabilities as shown in **Figure 2.** This model can also simulate fluid and proppant flow inside the fracture (Montgomery and Smith 2010). Nowadays, the temperature profile of fracturing fluid is incorporated to design concentration of gel-stabilizer, breaker, and proppant during stimulation treatment. Many models have been developed to replicate fluid movement inside fracture and proppant transport inside fracture for each fluid type. Recently, interaction of induced fracture and reactivated natural fracture on well productivity has been studied and incorporated to hydraulic fracturing models. However, some of these fracture models or simulations cannot closely duplicate the fracture geometry and conductivity in real hydraulic fracture because some physical phenomena, namely

hydraulic fracturing creation and post treatment efficiency of proppant pack, has not been fully studied.

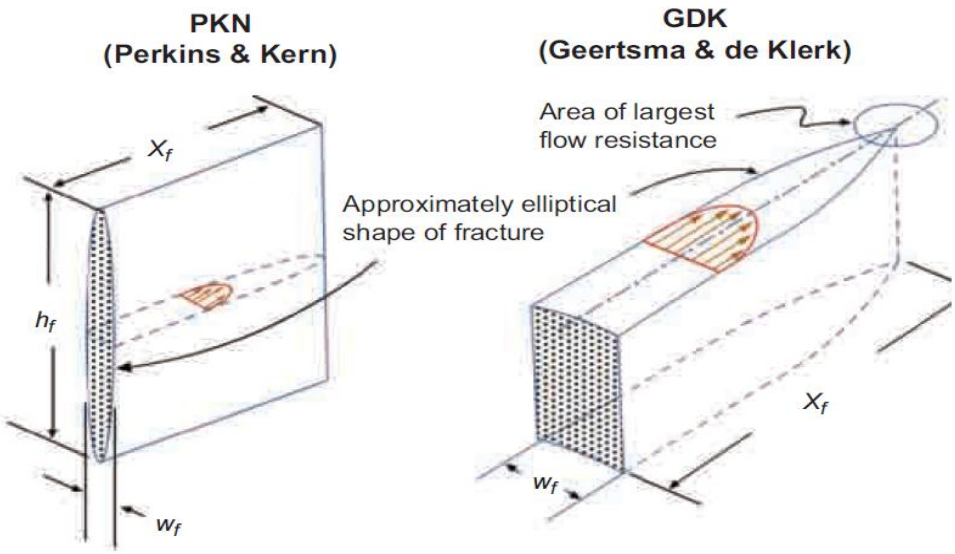

Figure 1. 2D Hydraulic fracture model (Montgomery and Smith 2010)

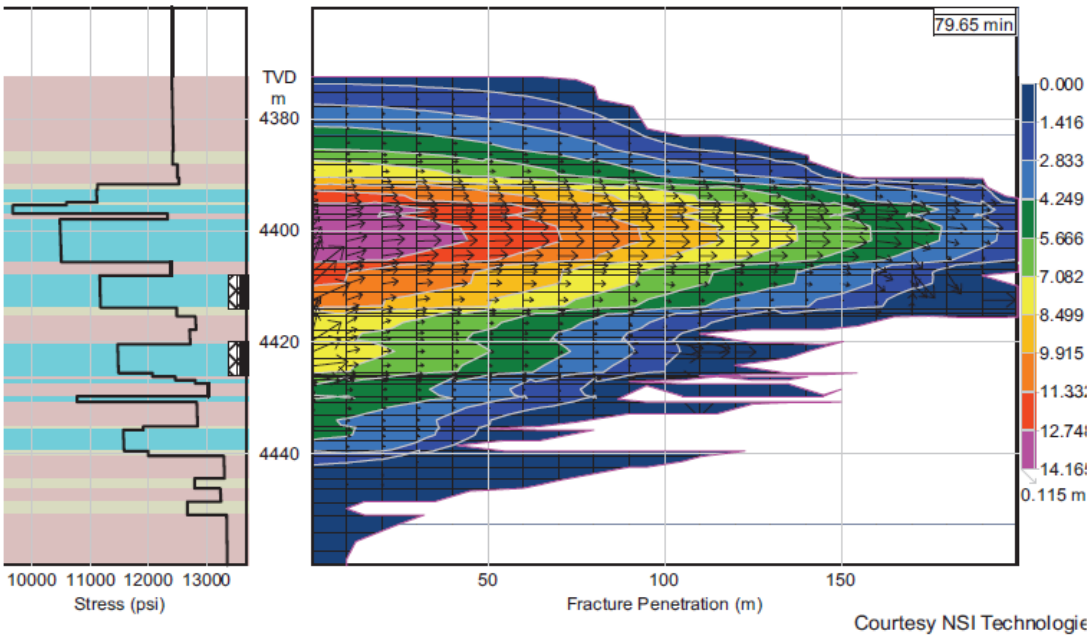

Figure 2. Fully grid finite element fracture model (Montgomery and Smith 2010)

To monitor hydraulic fracture geometry after treatment, microseismic events are studied and interpreted to use as a mapping tool for the presence of hydraulic fracture, or natural and induced fractures. Microseismic tools can provide information about fracture geometry, asymmetry, as well as geomechanical characteristics of rock (Warpinski 2014). Microseismic monitoring can be done by using both downhole and surface arrays. There are three main type of well monitoring: vertical, horizontal, and deviated wells. A vertical well is beneficial for evaluating the height growth of fracture while a horizontal well is useful for providing coverage data.

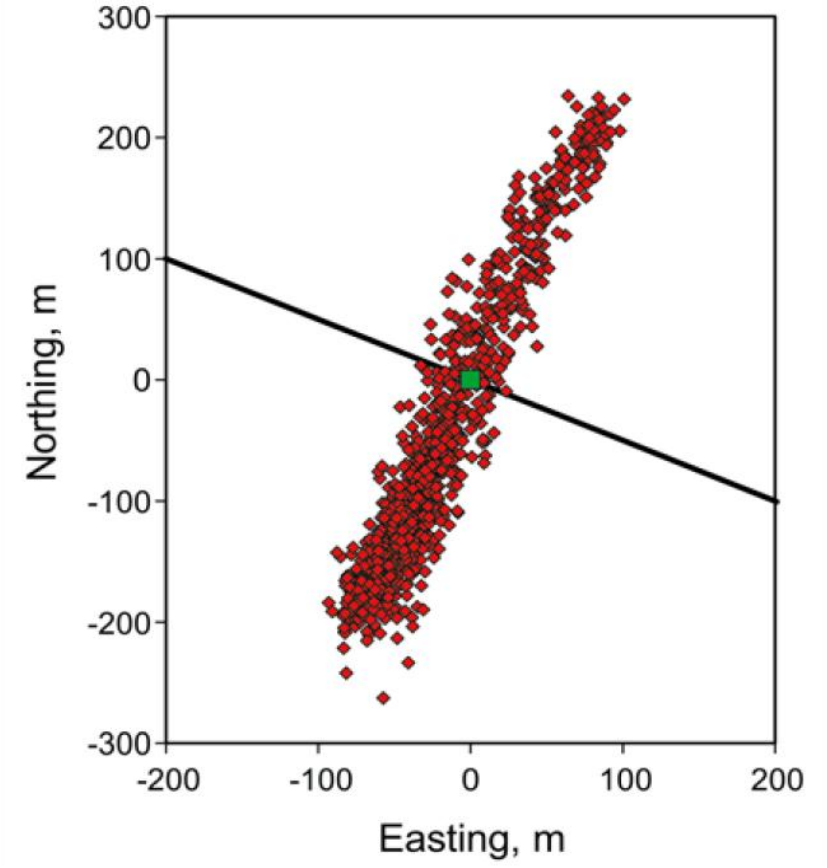

Figure 3. Map of planar fracture (Warpinski 2014)

Example of microseismic data interpretation is shown in **Figure 3** showing a map of planar fracture created in some direction. Also, **Figure 4** illustrates the side view map of multistage hydraulic fracturing in the Haynesville shale. It shows the height of fracture growth out of the productive zone. Hence, microseismic data is important to identify fracture geometry, induced fracture, and some stimulation operational problems.

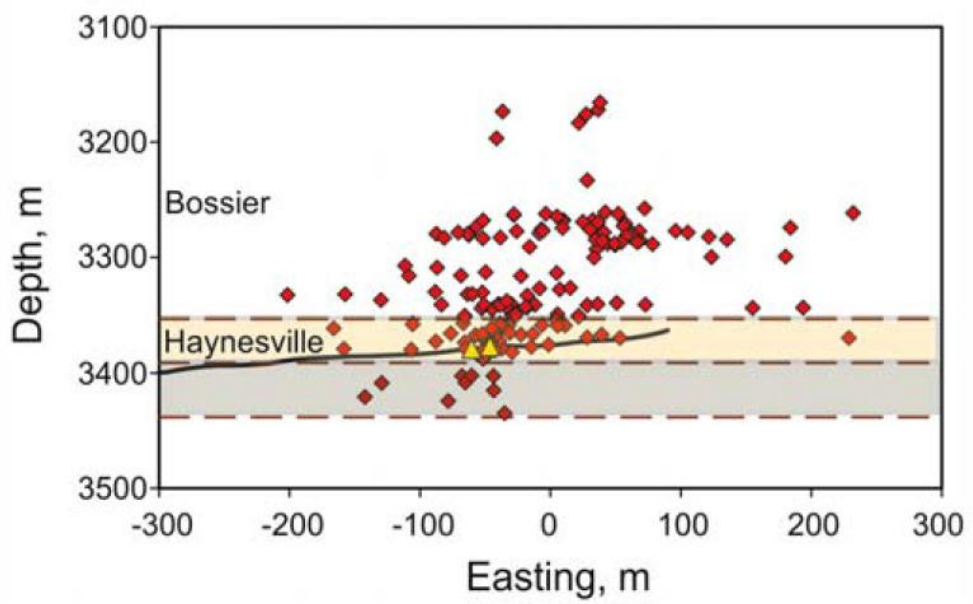

Figure 4. Side view map of hydraulic fracture showing significant height growth (Warpinski 2014)

1.1.2 Fracturing Fluid

Selection of fracturing fluid for unconventional reservoirs can be based on many parameters. Slick water or hybrid fracturing fluid systems may be used for brittle rock that can fracture easily to create highly complex fractures (Bi-wing and induced fracture). On the other hand, viscous fluid can be employed for ductile rock to create bi-wing fracture (Liang el al. 2015). SlickWaterFracs system (viscosified water base) can provide fracture with minimized gelling damage, but proppant transport capabilities are low. It is merely applicable for proppant concentration less than 2 ppa. Normally, a dune of

proppants at the bottom of a fracture are formed which limits vertical coverage (center and top zone will not have proppant and tend to collapse with time.) as shown in **Figure 5**. In addition, HybridFracs systems are developed to take advantage of either low or no gelling damage by SlickWaterFracs and viscous fluid system such as cross-linked fluid which provides good proppant transport capability (Manrique and Poe 2007). As a result, both vertical coverage and low gelling damage can be achieved as shown in **Figure 6**.

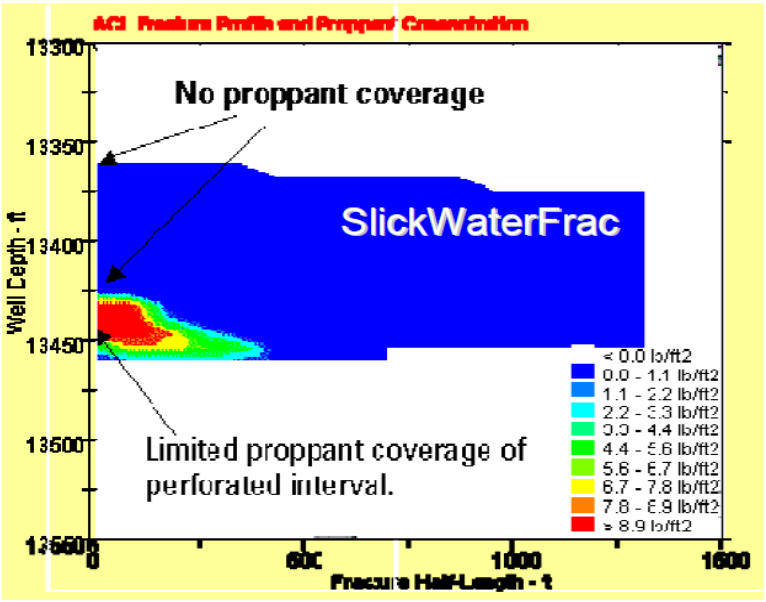

Figure 5. Fracture geometry and proppant concentration for slick water fractures (Manrique and Poe 2007)

On the other hand, other aspects of fracturing fluid selection is cost. Slick water fluid is apparently cheaper than conventional viscous fluid such as cross-linked fluid. There are key cost driving factors including 1) time required to complete stimulation, 2) volume of chemical needed, and 3) water volume. For slick water fractures, capability of transporting proppant inside a fracture is much lower so lower proppant concentration fluid is used. Therefore, the time required to complete a stimulation job and water volume is significantly higher than conventional fracturing fluid with the same amount of

proppant. Also, in the case of slick water systems, a high pump rate (50 to 80 bbl. /min) is used, so higher hydraulic horse power is required to execute the fracturing job (Yang et al. 2013). However, Conventional cross-linked fluid requires more chemical treatment.

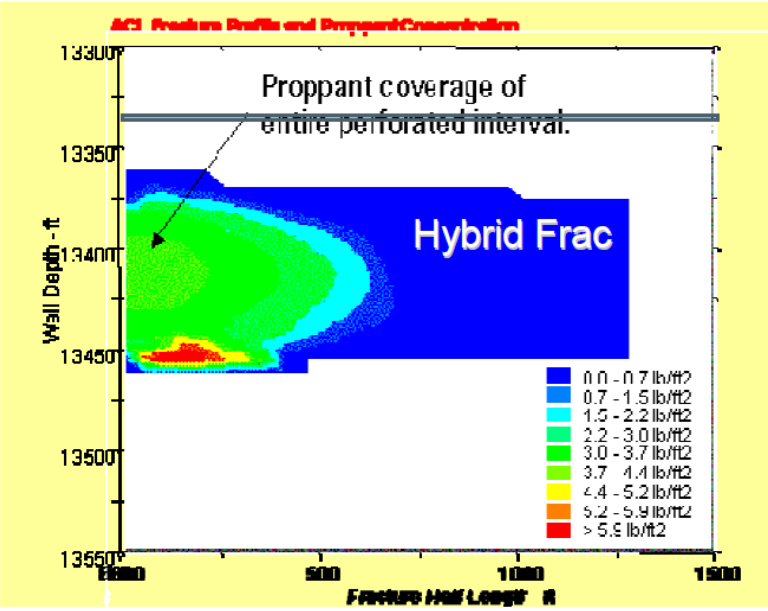

Figure 6. Fracture geometry and proppant concentration for Hybrid fractures (Manrique and Poe 2007)

There are some comparisons between slick water and conventional cross-linked fluid systems. For a conventional fluid system, wider fracture is obtained when compared to slick water system, even pumping at a high rate as shown in **Figure 7.** This illustrates that hydraulic fracture width is proportional to fluid viscosity and pump rate. As a result, there are some difficulties of placing high proppant concentration with slick water system. Pump width is important for placing proppant; however, the effective width after hydraulic pressure release and fracture tends to close is crucial for determining fracture conductivity. For conventional fluid systems, effective fracture width can be 50% less than pump width because of the distribution of proppant along the fracture consists of both fluid and proppant. Liquid itself cannot keep fracture to open and allow fracture to

close under confining stress. On the other hand, for slick water systems, proppant is settled rather than suspended in the fluid, forming proppant dunes as mention earlier. Therefore, at a proppant dune, high concentration of proppant allows effective width similar to pump (hydraulic) width. To summarize, for conventional fluid systems, pump width is larger, but effective width is smaller when compared to slick water system (Palisch et al. 2010).

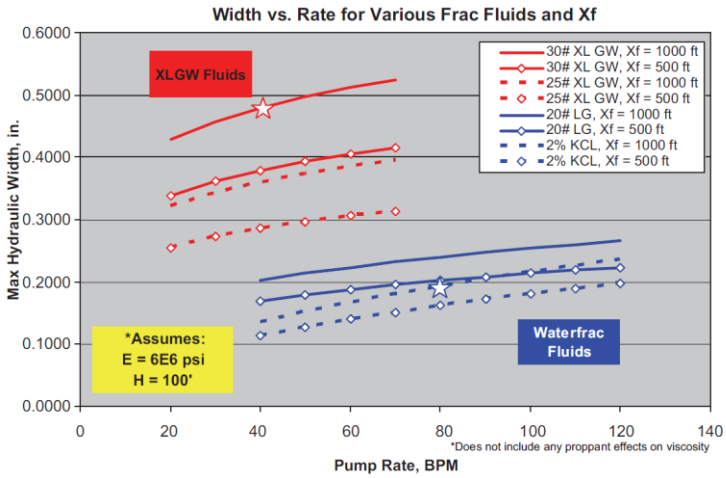

Figure 7. Hydraulic width of XLGW (Cross-linked) and Slick water fluid (Palisch et al. 2010)

As mentioned earlier, fracture complexity can be varied depending on both reservoir properties and fracturing fluid viscosity (leak off). Even though increasing fracture complexity can enhance reservoir contact, it might lead to poor connection between the fracture network and wellbore (Cipolla et al. 2008). For tight reservoir (microdarcy to nanodarcy), fracture complexity elevated the well productivity while the fracture network is detrimental in typical reservoirs (millidarcy to microdarcy).

1.1.3 Proppant

Proppant is material used to prop and create high conductivity flow path. Without proppant, fractures tend to close due to stress after the hydraulic pressure is released. Proppant can be classified into 3 tiers: uncoated sand, resin coated sand (RCS), and ceramic as shown in **Figure 8**. Physical properties such as proppant strength, shape, size uniformity, roundness and sphericity, and surface characteristics can dictate conductivity.

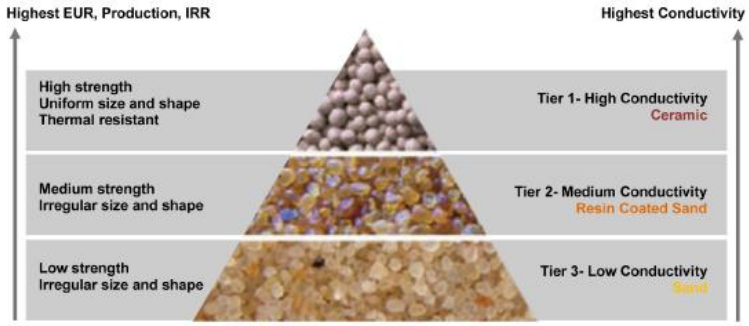

Figure 8. Hierarchy of proppant (Liang et al. 2015)

Proppant size can alter the fracture permeability. For instance, larger proppant possess higher permeability than smaller proppant when they are packed into a fracture. Most of proppant sizes are standardized by API. For example, 40/70 mesh proppant indicated by 90 % of proppant would fall through 40 mesh sieve and remain in 70 mesh sieve (Schubarth and Milton-Tayler 2004). Normally, hydraulic fracture starts with smaller proppant size at the beginning of slurry stage, and tail-in with larger proppant to maximize near wellbore conductivity.

The shape of proppant is a parameter that governs proppant conductivity. Ideally, proppant shape is spherical and non-angular. Higher sphericity and roundness of a proppant is expected to have higher conductivity. However, each tier of proppants has different shapes depending on how each proppant is acquired. For instance, natural

proppant has less sphericity than synthetic proppant. There are sphericity and roundness standards for proppant shape evaluation as shown in **Figure 9**.

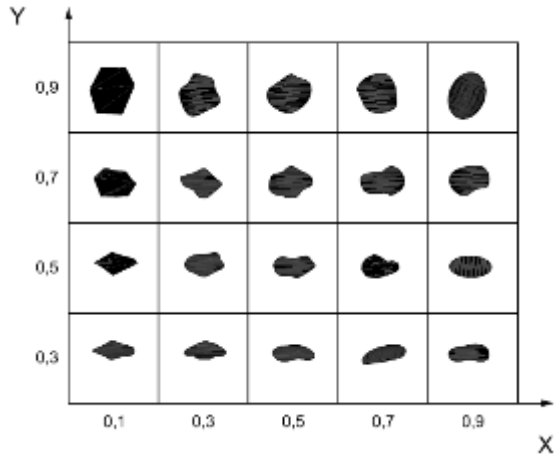

Figure 9. Measurement of sphericity (Y) and roundness (X) (Liang et al. 2015)

As mentioned earlier, proppant can be classified into 3 tiers which contribute to different physical properties and costs. Uncoated sand can be grouped as processed or high-silica content quartz sand. The term "sand" in this context does not mean sand natural mined without any processes. Some processes such as extracting, cleaning, and sizing is done before used as Frac-sand. Uncoated sand provides lowest conductivity and crushing resistance as well as highly angular shape compared to other tiers of proppant. However, uncoated sand is the most commonly used proppant because it is inexpensive and commonly available. Resin coated sand (RCS) was developed to capture fine that generates during proppant (sand) exposed to confining stress. There are two types of RCS including pre-cured and cured. The difference between these two RCS is the well needs to be shut in after fracturing job for cured RCS. This curing process allows consolidation of the proppant bed. Also, cured RCS is beneficial for proppant flowback reduction while pre-cured RCS can be employed to enhance stress resistance of sand (Palisch et al. 2010).

To characterize RCS, the glass transition temperature (T_g) is used as the upper performance limit of the particular type of resin. Above T_g, bulk property of resin is significantly changed (Dewprashad et al. 1993). Ceramic proppant is manufactured form sintered bauxite, kaolin, and magnesium silicate. It is more suitable for deeper wells because it possesses a higher crushing strength in addition to high sphericity, uniform size and shape. Therefore, porosity and permeability of proppant pack is higher than uncoated sand or RCS proppant pack. However, ceramic proppant is expensive when compare with other proppant tiers (Liang et al. 2015). It can be further divided into three category, based on density and alumina content including light weight ceramic (LWC), intermediate density ceramic (IDC), and high density ceramic (HDC). LWC possesses lowest alumina content and density while HDC have highest alumina content and density. With increased alumina content, proppant strength can be enhanced.

1.2 Conductivity Damaging Parameters

In this section, I will provide a list of conductivity damaging parameters. Fracture conductivity loss depends on several factors, such as physical properties of proppant, reservoir rock properties, fracturing fluid type, and well production schedule. Understanding the effect of these factors on conductivity loss can improve well performance prediction and fracturing design.

Proppant Crushing

One of the main concerns in successful hydraulic fracturing is strength and stiffness of proppant (Han and Wang 2014). Putting on production lead to decrease pressure inside the fracture and ascend net effective stress as shown in **equation 6.**

$$\sigma_{eff} = \sigma_T - \alpha P_p \quad (6)$$

Where σ_{eff} is net effective stress, σ_T is total stress from overburden, α is Biot's coefficient, and P_p is fluid pressure. As net confining stress increases, proppant tends to crush, and proppant sizes are decreased which lead to permeability drop. Crushing of proppant also generates fine particle, which can migrate and block the flow channel, as well as reduce fracture width (Gidley et al. 1995). Stress resistance of each proppant were tested via API standard conductivity test in the lab using the Cooke conductivity cell (API RP 61) with condition of 2 lb/ft^2 proppant loading, stress maintained for 15 min, 2 % KCl at 2 mL/min, and ambient temperature with steel piston. This standard is not sufficient to measure conductivity, so modified API test (ISO 13503-5) was introduced by changing steel piston to Ohio sandstone, increasing temperature to 150-250 F with 50 hours of stress maintained. **Figure 10** illustrates that same size proppant (40/70 mesh) with different materials can behave differently, resulting in varying permeability or conductivity on each applied stress due to different crushing strength, sphericity, roundness, and particle size distribution.

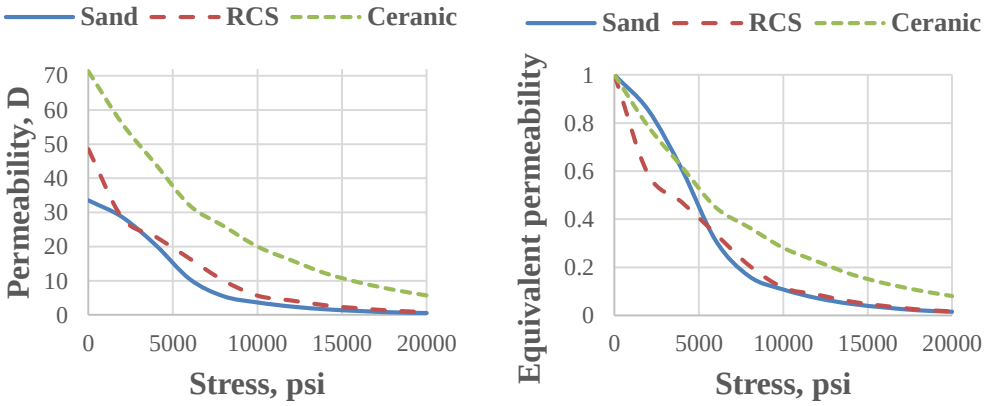

Figure 10. Effect of confining stress on proppant permeability for different proppant types (40/70 mesh)

However, modified API test (ISO 13503-5) is conducted at proppant concentration of 2 lb/ft^2 while real fracture for unconventional reservoir achieve 1 lb/ft^2 or lower. As a result, this test might not represent realistic proppant performance (Palisch et al. 2009). For instance, percentage of crush proppant are different when proppant concentrations change as shown in **Figure 11**. It shows that proppant tends to crush more with lower proppant concentration for all three types of proppant. The reason is exterior proppant suffers greater damage when compared with interior proppant, so proppant pack with lesser proppant concentration has higher portion of exterior proppant than that of higher proppant concentration pack. As a result, conductivity impairment of proppant pack with concentration less than 1 lb. /ft^2 is expected to be more severe compared to conductivity loss of API test.

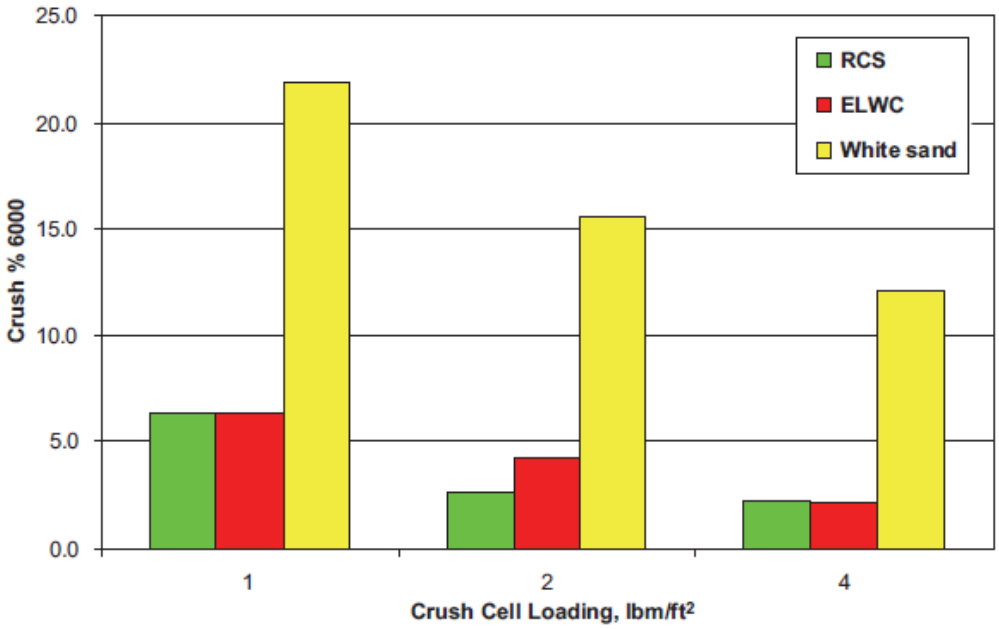

Figure 11. % Crush of three proppant types including sand, RCS, and ceramic at different proppant concentrations (Palisch et al. 2009)

Applied API Conductivity Test to Field Conductivity

Modified API (baseline) conductivity test is a good measurement for proppant conductivity under laminar conditions in the laboratory. However, conductivity was over estimated and real field conductivity is less than 10 % of lab-value (Vincent 2009). The reason of overestimating conductivity is the modified API test does not consider factors such as non-Darcy and multiphase flow, proppant embedment, gelling damage from gel residue of fracturing fluid, cyclic stress, fine migration and plugging, or proppant diagenesis. It has been suggested that all of these factors can significantly impair fracture conductivity and well productivity. Therefore, non-Darcy and multiphase flow, proppant embedment, gelling damage from gel residue of fracturing fluid, cyclic stress, fine migration and plugging, or proppant diagenesis must be considered in the fracture conductivity model. This conductivity is called as "**dynamic conductivity**".

Fine Migration and Plugging

After proppant crushing and formation spalling as proppant indents into fracture face under confining stress, generated fine particle migrates during production, and it can plug pore throats, which can significantly reduce proppant pack permeability (Weaver et al. 2007). As mentioned earlier, characteristic of fine particles of each proppant material can be different. For example, crushing of sand will generate high amounts of very fine particles. Resin-coated sand (RCS) might crush in similar fashion with sand, but resin coating encapsulates those fines, so RCS can prevent fine migration effectively. On the other hand, ceramic proppants crush in different fashion. Breaking particles are much bigger than that of sand, so it is more difficult for breaking particles to migrate and plug any pore throat (Ghosh et al. 2014). Therefore, different crushing manner will generate

different degrees of fine migration and plugging. One important factor of particle migration and plugging is fine particle size relative to pore throat size. There are three possible scenarios: 1) particles are too large to pass through pore throats, 2) particles are small enough to completely pass through pore throats, and 3) particle are small enough to pass through pore throats but it large enough to block some small pore throats.

Abundant research has studied the movement of particle in porous media. For example, (Saucier 1974) formation sand cannot penetrate into proppant pack if proppant grain are six times larger than formation sand diameter, so it can be confirmed that particle larger than 15% of proppant size are immobile based on assumption that proppant shape is perfectly sphere without crushing. For large breakage particle, it is difficult to rearrange and migrate, which does not significantly damage proppant pack. Also, very small fine particle relative to proppant size can migrate through proppant pack without any damage. For instance, 300 mesh particle can completely flow through 20/40 proppant pack without plugging. However, fine production can provide negative impact on wellbore and surface facility, such as wellbore integrity and operational problems. Intermediate size fine particles have the highest potential to considerably decrease conductivity via plugging process. Once particles can pass through the proppant pack, its size is large enough to plug small pore throats (Palisch et al. 2009).

Figure 12 shows permeability change with time for different types of proppant in a shale sample. Sand exhibits notable permeability drop (99%), while Ceramic shows 70 % permeability reduction after 10 days. However, RCS shows no permeability drop due to the fine particle capturing capability (Ghosh et al. 2014).

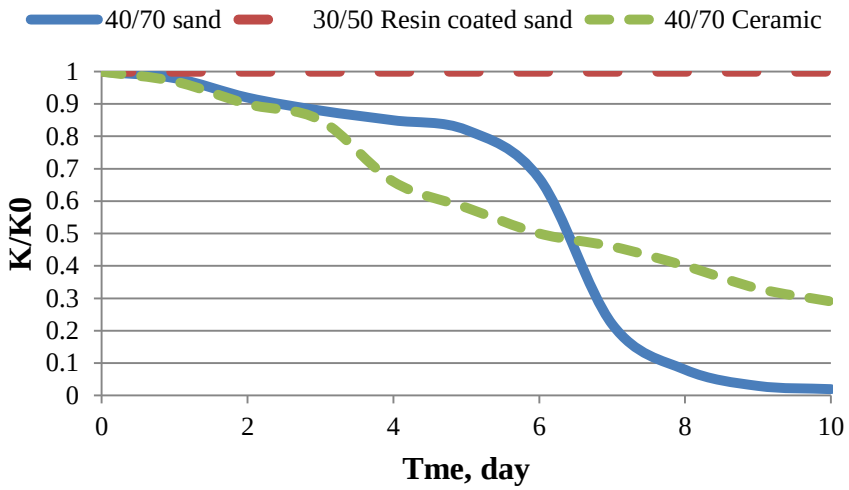

Figure 12. Permeability loss with time for different types of proppant (Ghosh et al. 2014) (k/ko is ratio of permeability at specific time over initial permeability.) (Experiment procedure and condition are shown in Appendix B1.)

In addition, extrapolating this result to other proppant size should be done with caution. The reason is that different size of proppant will provide different pore structure and fine particle sizes under stress. For example, 20/40 mesh sand has bigger pore throats compared to 40/70 mesh. Therefore, the degree of particle migration and plugging are altered.

Proppant Embedment

Indentation of proppant into fracture surfaces leads to fracture aperture loss. This mechanism varies from one fracture to other depending on the Young's Modulus (soft or hard) of rock, mineral composition, temperature, pressure, confining stress, fracture fluid exposure time, fracture fluid type, and proppant type. Soft rock (low Young's Modulus) leads to more indentation when compared to hard rock. The longer a rock is exposed to fracturing fluid, the rock tends to be softer and higher indentation is expected as shown in **Figure 13** (Denney 2012).

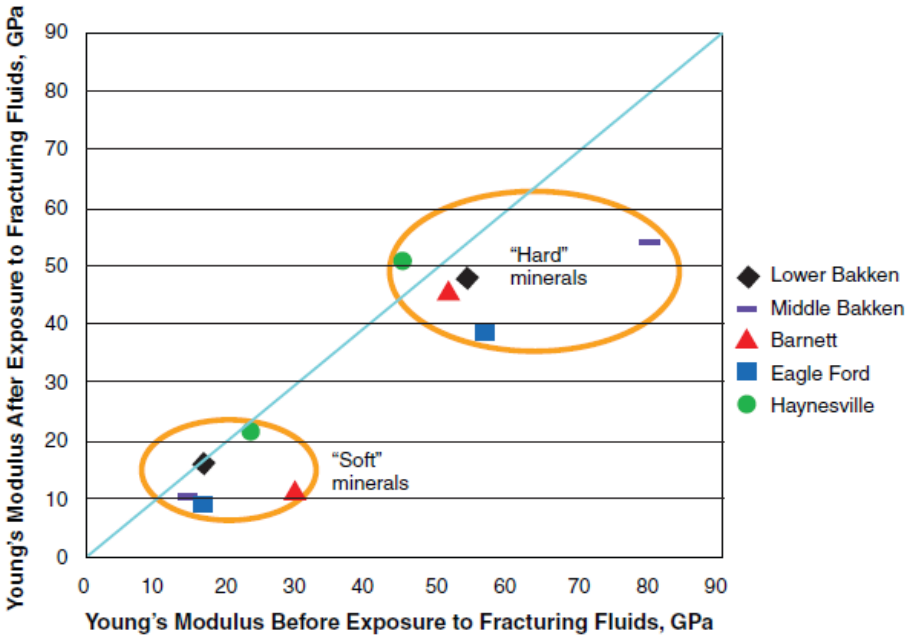

Figure 13. Rock Young's Modulus before and after expose to fracturing fluid for 48 hours at 300 ˚F (Denney 2012)

For example, Young's Modulus of Eagle Ford shale is decreased as much as 51 % after 15 days of fluid exposure. With the association of high temperature, decreasing of Young's Modulus is more severe. **Figure 14** (Alramahi and Sundberg 2012) illustrates that softer rock (higher clay content) exhibits more proppant indention, and proppant embedment gradually increases as increased confining stress for all cases of rock. Also, the type of proppant can dictate the degree of proppant embedment. Weaver et al. (2005) illustrate proppant embedment of each proppant type as shown in **Figure 15**. Ceramic proppant exhibits higher embedment than sand. However, RCS almost eliminates proppant embedment. Explanation for this phenomena is the thin coating resin provides higher contact area which helps distribute stress loads.

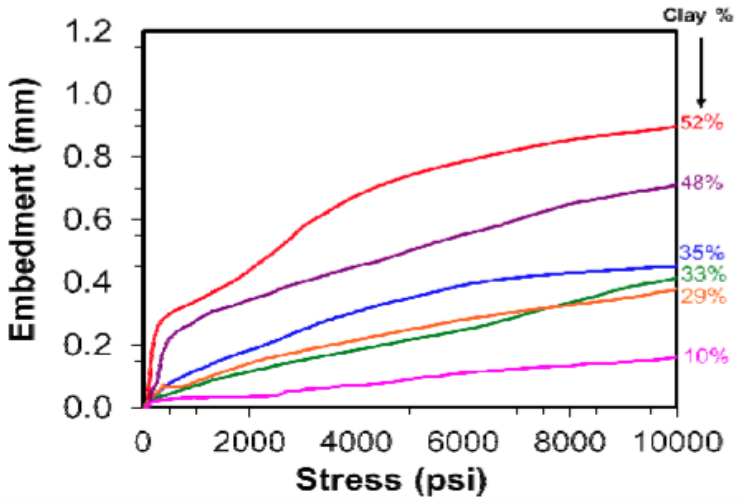

Figure 14. Degree of proppant indentation based on stress and rock composition (Alramahi and Sundberg 2012)

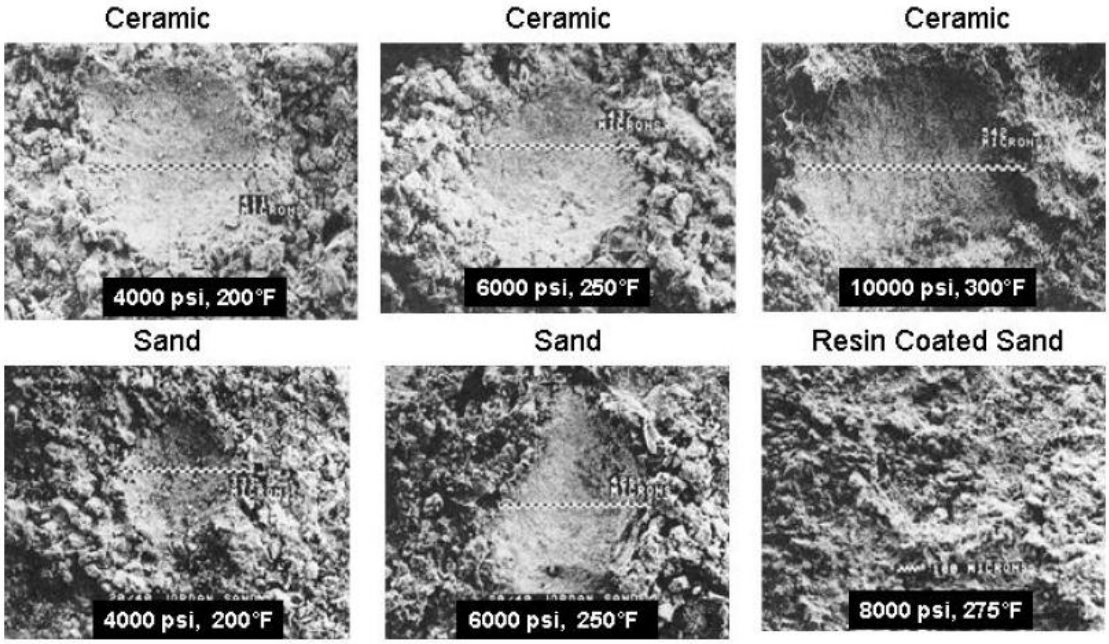

Figure 15. Craters left by 20/40 mesh of each proppant into Ohio sandstone at various confining stresses and temperatures (Weaver et al. 2005)

Proppant Diagenesis

Degradation of proppant packing via diagenesis reactions leads to porosity loss, and significantly reduces conductivity over time. The term "diagenesis" is well known by geologists in the formation of the geologic formations. Under high stress and temperature, contact points between grains of materials are dissolved into the surrounding formation. As this process continues, solutions become supersaturated and precipitates out of solution in the crystal form (Weaver et al. 2007). In fact, reservoirs can be considered being in an equilibrium state. After the drilling or fracturing process, new materials, such as fracturing fluid and proppant are introduced to this formation, which lead to a non-equilibrium state, and allow diagenesis reactions (Weaver et al. 2009).

In proppant packing as shown in **Figure 16** (Yasuhara et al. 2003), compression forces on the contact point between two proppants are very high because of the smaller contact area. This contact point is the weakest point that can be dissolved, leading to an increase in concentration of ions in the solution. Subsequently, dissolved material migrate and diffuse to other supersaturated areas. As a result, this solution starts to precipitate, generating new particulate filling material.

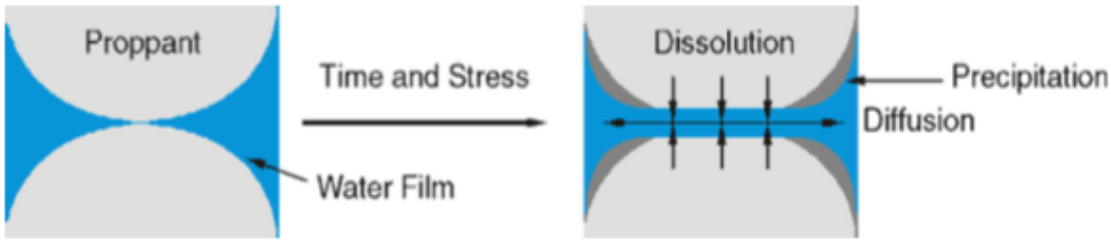

Figure 16. Pressure solution mechanism via compaction process (Yasuhara et al. 2003)

(Weaver et al. 2007) noticed that the presence of a filling material in proppant packing at 6000 psi confining pressure and 225 °F by the using SEM-EDS technique as shown in

Figure 17. Also, the Si/Al ratio of this filling material is 4.9, which is the intermediate value between ceramic proppant (0.9) and Ohio sandstone (8.4). Weaver noticed about 50-90 % permeability drop of proppant packing as a result of diagenesis reaction.

Weaver mentioned that coating proppant with resin (surface modifying agent) can significantly reduce diagenesis reactions because the coating material prevents contact between fluid and proppant.

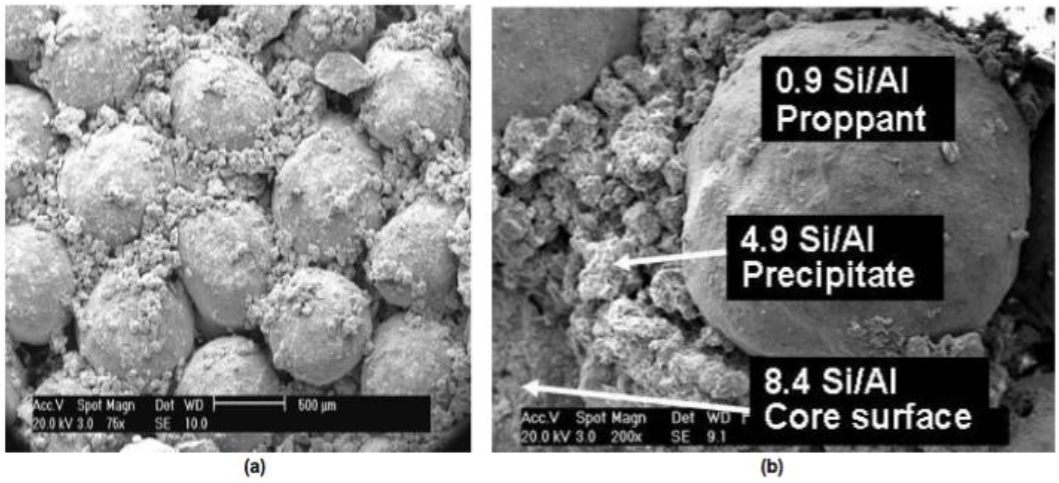

Figure 17. SEM image of 20/40 mesh ceramic in Ohio sandstone formation (Weaver et al. 2007)

Proppant Transport and Placement

Prediction of proppant placement is one of the most important parameters in hydraulic fracturing design. In the proppant laden stage, fracturing fluid and proppant are pumped into a fracture; the role of fracturing fluid in this stage is to distribute and deliver proppant into the right place of the fracture. Proppant placement contributed significant effects on fracture geometry and conductivity in each zone of fracture. In hydraulic fracturing designs, fracturing fluid can be classified into two main types. First, non-cross-linked fluids, such as slick water fracturing systems, have low viscosity and particle settling is

considerable. Second, cross-linked fluids possess high viscosity and particle settling is not important. However, convection and encapsulation dominate proppant placement (Clark 2006). Non-cross-linked fluid, particle (proppant) settling is governed by Stoke's particle settling velocity for single particle in static condition as shown in **Equation 7**.

$$v_t = \frac{d_p^2(\rho_p - \rho_f)g}{18\mu_f} \quad (7)$$

Where d_p is proppant diameter, ρ_p is density of proppant, ρ_f is density of fluid, g is acceleration of gravity, and μ_f is viscosity of fluid. For slick water systems, viscosity of fluid is low (< 10 cp), so small proppant size or light weight proppant is suitable. However, Stoke's particle settling velocity relied on some assumptions that do not occur during hydraulic fracturing.

1. Fluid is moving instead of static.
2. Proppant particle settling near fracture face (wall) is lower than that of in middle of fracture (no wall effect).
3. Particle interaction can enhance or reduce settling velocity. For example, clustered or agglomerated particles can increase settling velocity or hindered settling can reduce particle settling.

Therefore, predicting proppant transport and placement using Stoke's particle settling velocity is inadequate, and complex mathematical models have been developed to address its limitation. For a slick water system, proppant settles very fast, forming a proppant bank which is immobilized. The proppant transport can be dictated by movement of the proppant bank with three transport mechanisms: suspension, reputation, and saltation (Mack et al. 2014). At low velocity, proppant does not move. Proppant rolls along the

surface of the proppant bank at higher velocity (reputation). Lastly, at even higher velocity, proppant jumps off the bank into flow stream (Saltation).

Cross-linked fluid, proppants travel with the fluid, but there are two-mechanisms controlling the proppant placement. Convection is movement of fluid due to a density difference, and encapsulation is the absorption of long chain polymers, according to the dictionary of Petroleum exploration, Drilling and Production. One of the earlier works focused on convection topic is Clark et al. (1977) indicated that clustering or agglomerating of particles can increase settling velocity. Particle agglomerate with others results in a larger cluster which can settle faster. This is called "cluster settling velocity". Cleary and Fonseca Jr. (1992) indicated that convection is the most important parameter in fracturing design associated with non-Newtonian fracturing fluid, and convection is related to fracture width. Barree et al. (1994), bulk density gradient is the crucial factor on the slurry velocity profile. Shah and Asadi (1998) indicated that increasing viscosity of the lower medium can prevent convection and encapsulation, and increase fracture width exponentially, enhancing convection.

Clark (2006) investigated proppant transport in elliptical shaped fractures, providing different results from previous slot fracture studies. There are two acting forces incorporated, including horizontal forces that moves the slurry through length of slot, and gravitational force that drags particles to the bottom of a slot. Introducing dimensionless **Equations 8 and 9** used to quantify degree of convection.

$$Nc = \frac{12q\mu}{gw^3\Delta\rho} \qquad \text{Newtonian fluid (8)}$$

$$Nc = 2\left(4+\frac{2}{n}\right)^n \frac{Kq^n}{gw^{2n+1}\Delta\rho} \qquad \text{Power-law fluid (9)}$$

Where Nc is convection number, q is injection rate divided by height, μ is viscosity of injected fluid, g is gravitational force, w is slot(fracture) width, Δρ is density difference between injected fluid and fluid in slot, k is flow consistency index, and n is behavior index. Clark (2006) indicated that convection will dominate if Nc is less than one, and vice versa. **Figure 18** indicates that proppant distribution is better in the case of higher Nc due to less convection effect. On the other hand, in the case of high convection (a), proppant tends to accumulate at the bottom part of the fracture, which leads to lower proppant coverage and fracture conductivity in the fracture tip area.

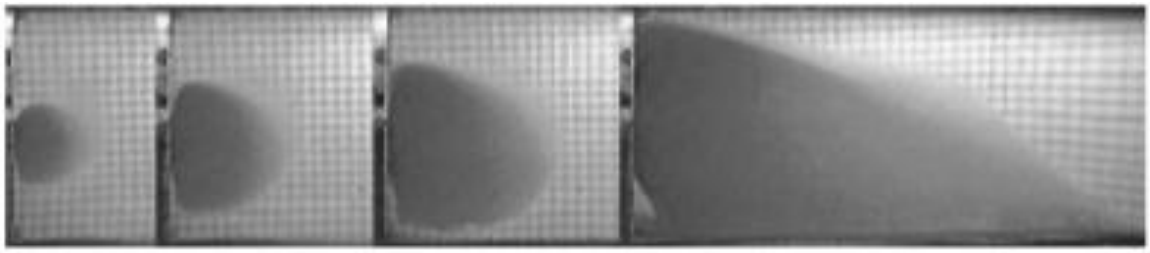

(a) Convection number Nc = 0.75

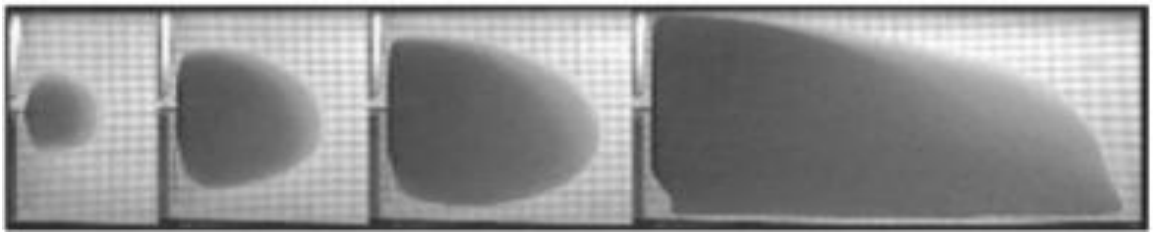

(b) Convection number Nc = 1.50

Figure 18. Time series of proppant transport (Clark 2006)

From **Equation 8 and 9**, small changes in slot width can contribute to a significant change in Nc value. Therefore, fracture properties (non-uniformities) strongly influence the proppant transport and placement. Anisotropy and stress variation in reservoir conditions can cause non-uniformities of the fracture from top to bottom and the wellbore to tip, so proppant placement is difficult to predict with such uncertainties.

Gelling Damage

To provide a good proppant placement in hydraulic fracturing process, viscous fracturing fluid such as cross-linked gel is required. After treatment, a breaker is injected to break-up polymer networks and reduce fracturing fluid viscosity, which allows fluid flow back. Breaker used in clean-up operations can be an oxidizing agent, organic acid, or enzymes. However, this clean up procedure is ineffective, especially in the fracture tips region, leaving gel residue to cover both fracture face and proppant pack. As a result, fracture conductivity and effective fracture length can be much lower than expected. In high polymer loading fracture fluids, conductivity can decrease up to 80 % of its original value. An example of gel residue is shown in **Figure 19** (Cooke Jr. 1975).

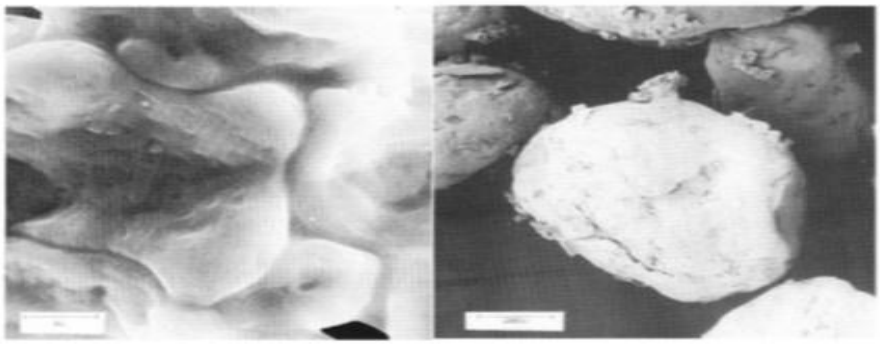

Figure 19. Gel residue (left) and sand covered by gel residue (right) (Cooke Jr. 1975)

Breaking efficiency depend on polymer and breaker type, initial concentration, reaction time, or reservoir properties. For instance, reservoirs with high permeability or natural fracture, gelling damage is more severe due to the low-pressure gradient in fracture and breaker leak-off, leading to decreased breaker concentration (Han et al. 2015).

Cyclic Stress

Rational for alternately producing or shut in hydraulically fractured wells is often due to fluctuation in market demand, well maintenance, or government regulations. Proppant pack experiences fluctuated closure stresses that allow additional proppant crushing and redistribution. Also, according to laboratory results, fine particles are increased as cyclic stress increases. As a result, cyclic stress can deteriorate proppant conductivity over a number of cyclic stresses. Stephens et al. (2007) indicated that cyclic stresses also change the size distribution of proppant, and the most considerable change of size distribution is during the first five stress cycles. According to Berg's equation as shown in **Equation 10,** there is a relationship between median particle diameter and permeability of sandstone formations.

$$K = 5.1 \times 10^{-6} n^5 d_{50}^2 e^{-1.385(d_{90}-d_{50})} \quad (10)$$

Where n is porosity, d_{50} is the median particle size (mm), d_{90}-d_{50} is difference between 90^{th} and 50^{th} particle size (mm). In fact, cyclic stress can reduce pack porosity and proppant particle size, so proppant pack permeability is descended considerably as suggested by **Equation 10**.

Ouabdesselam and Hudson (1991) indicated that uncoated sand experiences higher permeability loss than ceramic proppant over stress cycles due to possessing lower crushing resistance. Proppant pack width and conductivity reduction caused by (1) mechanical failure of fracture face (spallation), (2) additional proppant embedment, or (3) mechanical failure of proppant. Cyclic stress is more pronounced when a reservoir formation is soft, as shown in **Figure 20**. Also, Ouabdesselam and Hudson (1991) suggested proppant pack width reduction in real fractures are more severe than that of flat

formation core plate (laboratory). Ouabdesselam and Hudson (1991) also mention that cyclic loading affects the structural integrity of the proppant. Larger proppant size experiences higher cyclic loading effects than smaller proppant. Stephenson et al. (2007) concluded that the behavior of proppant over a stress cycle is dependent on proppant material, proppant concentration, and rate of loading/unloading during stress cycles. Conductivity loss of proppant pack caused by both decreased permeability and reduced packing width. From **equation 10**, the retained permeability over a number of stress cycles is calculated for various types of proppants, as shown in **Figure 21.**

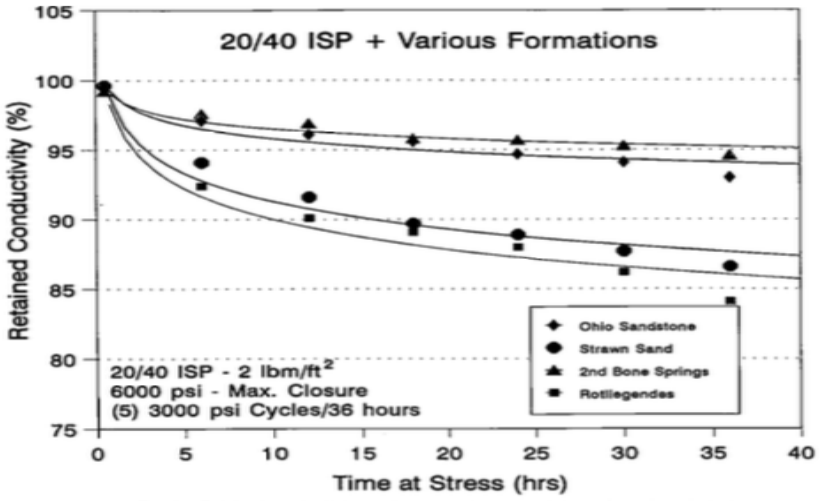

Figure 20. Retained conductivity of various sandstone formation over 5 stress cycles (Ouabdesselam and Hudson 1991)

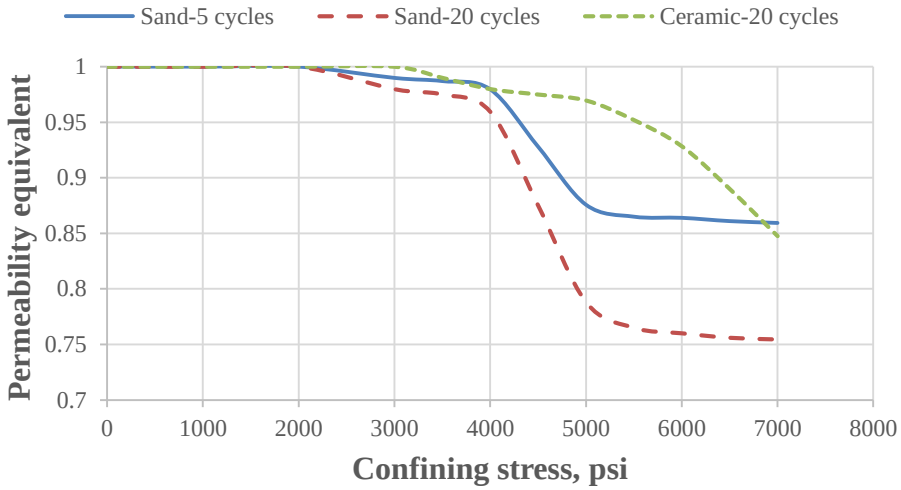

Figure 21. Retained permeability over number of cyclic stresses for each proppant type (Derived from Schubarth and Milton-Taylor (2004) data) (Experiment procedure and condition are shown in Appendix B2)

1.3 Literature Review

1.3.1 Improving Production in the Eagle Ford Shale with Fracture Modeling, Increased Conductivity and Optimized Stage and Cluster Spacing along the Horizontal Wellbore

Bazan et al. (2010) perform history matching for well A of Eagle Ford shale (283 ft of pay interval) which was completed with 10 stages of fracturing with varied fracturing fluid such as slick water, and linear gel. 40/80 lightweight ceramic is used as a proppant, and proppant concentration during the stage ranges from 0.25 to 1.5 lb. /gal. Total amount of proppant and fracturing fluid are about 250,000 lb and 11,300 bbl. per stage respectively. With the calculated bottomhole pressure, production history matches are carried out for 9 month periods as shown in **Figure 22.** Author assumes that fracture conductivity is uniform throughout the fracture length. The result of the history matches are shown in **Figure 23,** indicating that fracture conductivity is 4.19 mD-ft which is typically very low compared to Baseline conductivity. This example shows the difference

between the value of Baseline conductivity from laboratory measurement and realistic or dynamic conductivity at downhole condition.

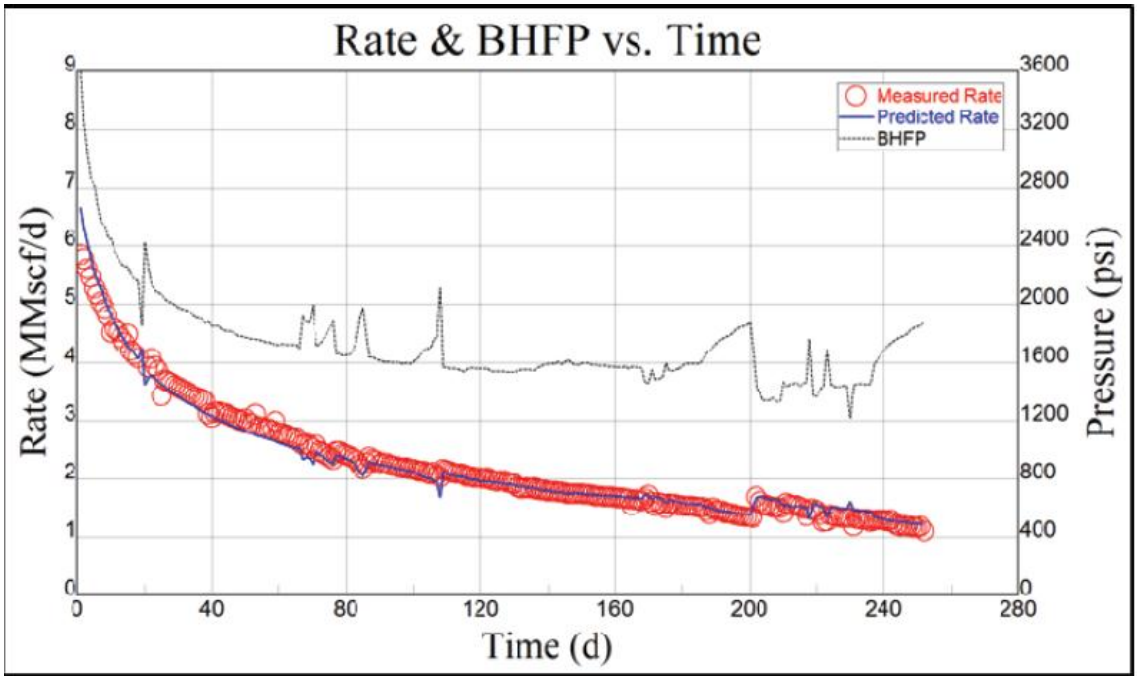

Figure 22. Measured and predicted gas flow rates for well A in a 9 month period (Bazan et al. 2010)

Number of Transverse Fractures	**10**
Propped Half-Length, x_f, (ft)	245
Dimensionless Conductivity, C_{fD}	261
Conductivity, $k_f w_f$, (mD-ft)	4.19
Permeability, k, (nD)	65.6
Reservoir Capacity, kh, (mD-ft)	0.019
Equivalent. Fracture Skin, S	-5.88
Choked Skin, S_{ch}	0.0198
Std. Deviation (MMscf/d)	0.14
Error (%)	4.5

Figure 23. Parameter derived from history match (Bazan et al. 2010)

1.3.2 Hydraulic Fracture Optimization in Unconventional Reservoir

Saldungaray and Palisch (2012) illustrated overall impact of damage mechanisms on the conductivity at downhole condition. Conductivity loss is more than 90 % as shown in **Figure 24** and individual damage mechanisms can be varied depending on proppant type. Realistic conductivity is far less than conductivity measured in the laboratory. Hence, without taking into account of this conductivity reduction, considerable production can be deferred or not be recover in the worst case.

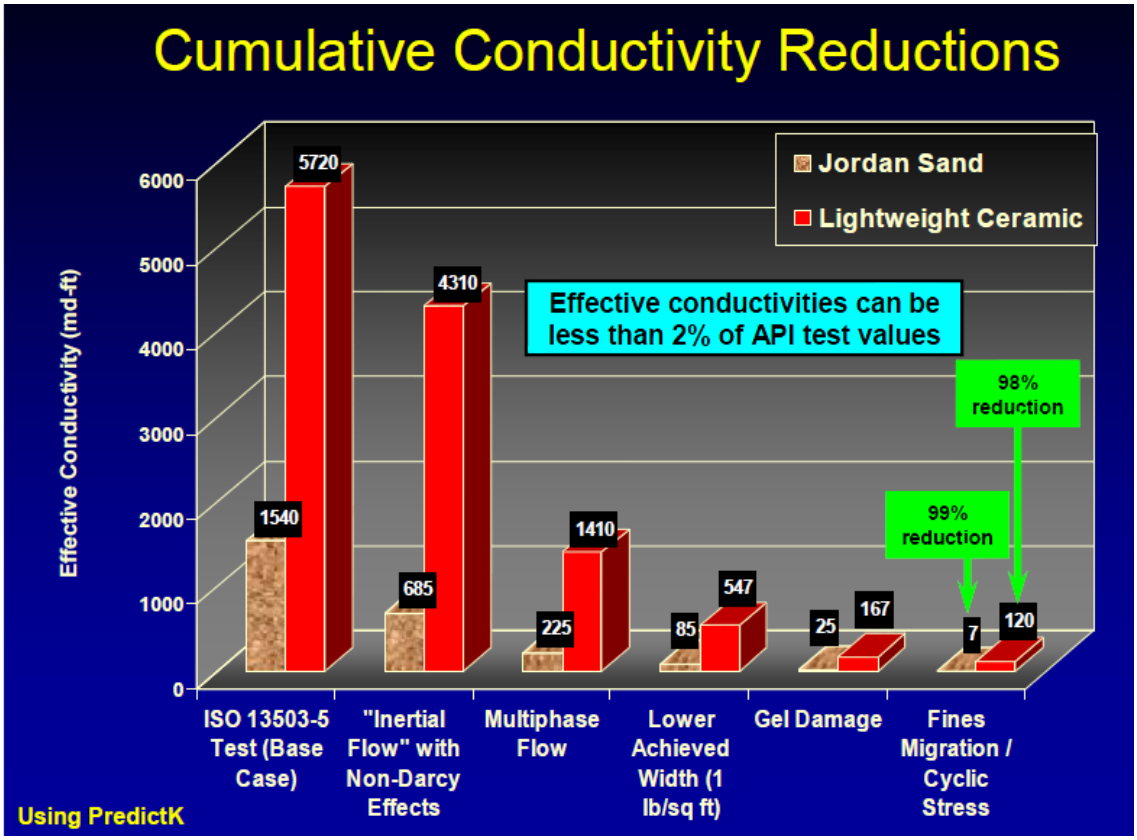

Figure 24. Reduction of fracture conductivity due to damage parameters (Saldungaray and Palisch 2012)

Saldungaray and Palisch (2012) mentioned that fracture with very low fracture conductivity (Dynamics conductivity) for micro and Nano Darcy scale in unconventional reservoirs is still effective because fracture permeability is significantly better than

reservoir permeability. However, fracture flow capacity is not optimized (Fcd is lower than expected.). There are plenty of ways to improve conductivity, such as increasing proppant concentration and size, changing proppant type, or using a different fluid that can reduced gel damage. However, negative effects should be considered; for example, attempting to increase fracture permeability by enlarging proppant size can increase settling velocity of proppant and cost. Saldungaray and Palisch (2012) also proposed 3 steps of proppant selection.

1. Calculate realistic conductivity at reservoir condition and predict expected production for particular proppant type. (This step can be done by using fracture propagation model coupled to reservoir simulator.)
2. Identify cost and well productivity increased for each proppant and select proppant which maximizes economic benefit.
3. Validation of predicted production with actual field production.

Saldungaray and Palisch (2012) shows an example of effect of improving proppant quality on well productivity of middle Bakken oil well with 80 ft. pay thickness. Average porosity is 5 % and permeability is 0.04 mD. Operator performed a test to evaluate the benefit of increasing conductivity. 10 wells were stimulated using 20/40 low density ceramic, and the other 12 wells were stimulated by using 20/40 sand with similar fracture design and completion. After 22 months, the cumulative production of ceramic proppant wells have 34% more hydrocarbon than sand wells, which is $1,500,000 incremental profit while incremental cost is $300,000 from using ceramic rather than sand as proppant as shown in **Figure 25**. Assumption is price of oil and gas are $75/bbl. and $3.5/MCF respectively.

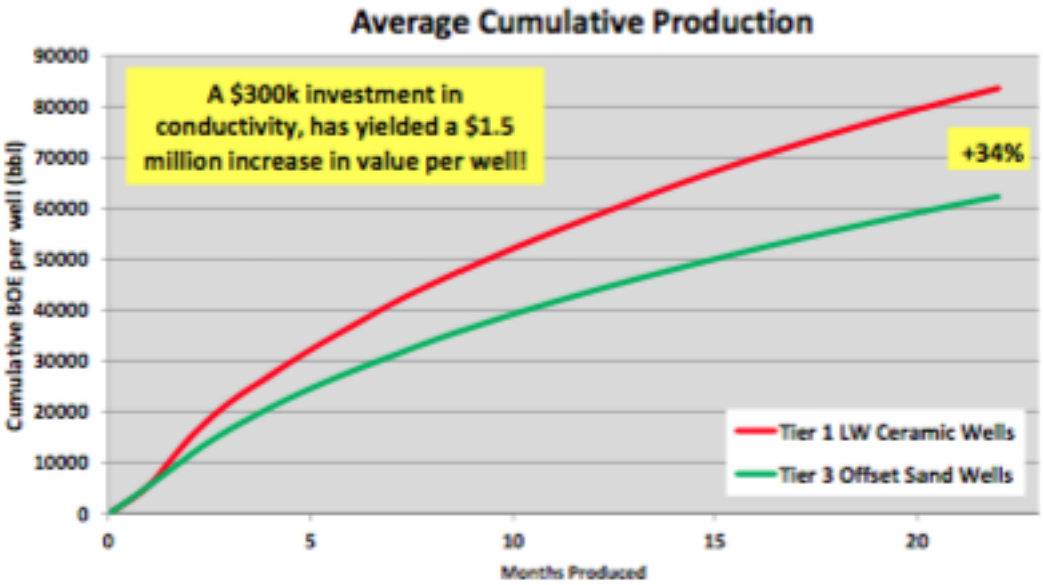

Figure 25. Oil cumulative production for different proppant type well (Saldungaray and Palisch 2012)

1.3.3 Design Flaws in Hydraulic Fracturing

Economides and Wang (2010) indicated that using Unified Fracture Design (UFD) approach has limitations. For example, using better proppant (higher k_f) will result in smaller width and longer fracture for the same given amount of proppant. Authors investigated the effect of gel damage on well performance in varied reservoir permeability as shown in **Figure 26**. The vertical axis is ratio of productivity index between damaged and undamaged proppant pack and horizontal axis is the degree of gel damage. For reservoir with 0.01 md, productivity index reduction is less than 10 % even at 75 % gel damage. On the other hand, reservoir with 1 md, well performance is reduced almost 40 % at 75 % gel damage.

Economides and Wang (2010) also investigated the effect of leak off damage which is penetration of fluid into reservoir rock from fracture face. It can be quantified by using the Cinco and Samaniego skin, sff as shown in **Equation 11**.

$$S_{ff} = \frac{\pi b_s}{2x_f}\left(\frac{k}{k_s} - 1\right) \quad (11)$$

Where, b_s is penetration of damage, and k_s is damaged permeability. However, Aggour and Economides (1996) indicated from experimental results that cross-linked fluid will not penetrate into formation when reservoir permeability is less than 600 md, and linear gel fluid will not penetrate into formation when reservoir permeability is less than 5 mD.

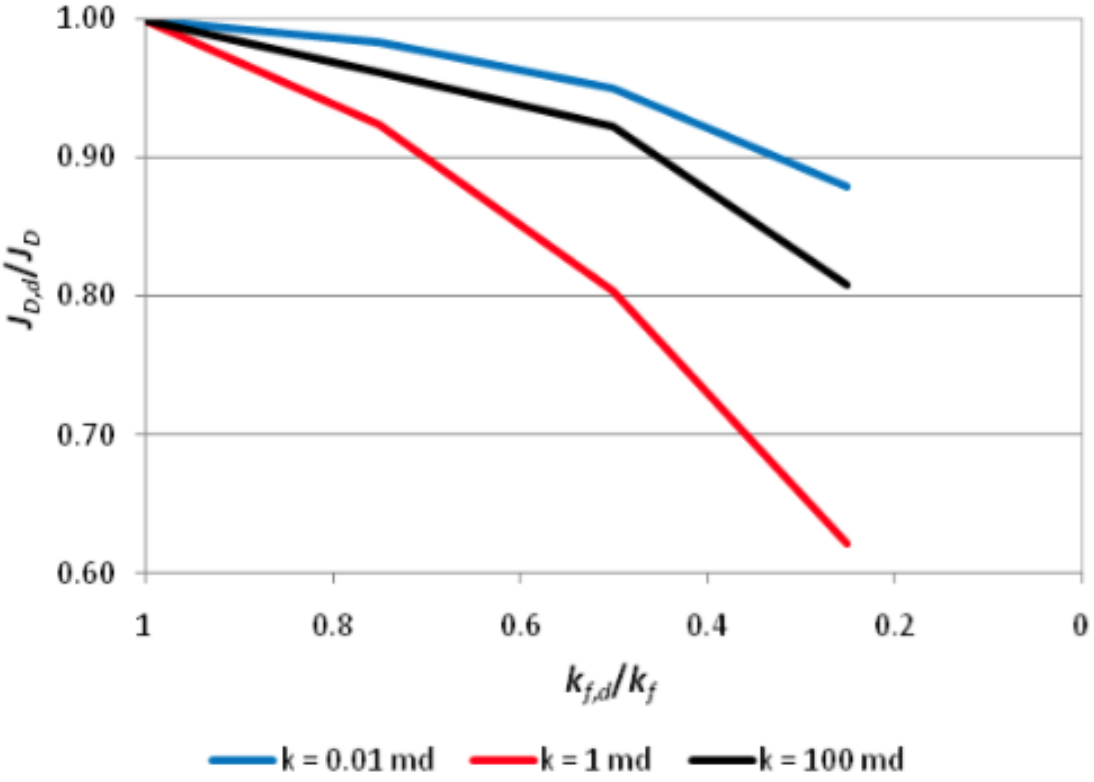

Figure 26. Effect of gel damage on well performance based on UFD approach (Economides and Wang 2010)

Chapter 2: Loss of Fracture Conductivity

Fracture geometry and conductivity can be varied as discussed in the previous chapter. Arbitrary created hydraulic fracture (Fracture with uniformed conductivity) is not sufficient to mimic real hydraulic fracture behavior. Hence, hydraulic fracture models are necessary to simulate fracture properties. Also, there are several factors that impact fracture conductivity, and factors are varied depending on type of proppant, fracturing fluid, and etc. This factor can be either function of time or stress. Therefore, laboratory-base measurements are gathered and introduced into fracture conductivity loss models. Some assumptions are made due to the limitation of data available.

2.1 Modelling Hydraulically-Created Fracture

In this work, a tight oil reservoir from the Niobrara formation is studied. I use the fracturing simulator of Fracpro (Fracpro, 2012) to model and simulate conventional symmetric bi-wing fracture. Due to stress anisotropy and shadowing, depletion of pressure in the previous producing well region, and presence of natural fracture, however, asymmetric and non-uniform fracture geometry is expected (Sahai et al. 2013) and (Mata et al. 2014). For the sake of simplicity, bi-wing fracture is a reasonable approximation for tight oil reservoir fracture. Additionally, our assumption is that rocks behave in a ductile manner and high viscosity fracturing fluid is used that can minimize leak off, so the fracture configuration is not complex (less induced fracture) (Quintero and Devegowda 2015). Effects of rock fabric on fracture geometry and complexity are shown in **Figure 27.** More ductile rocks tend absorb more energy without breaking, which creates less fracture complexity and traverse induced fracture compared to brittle rock.

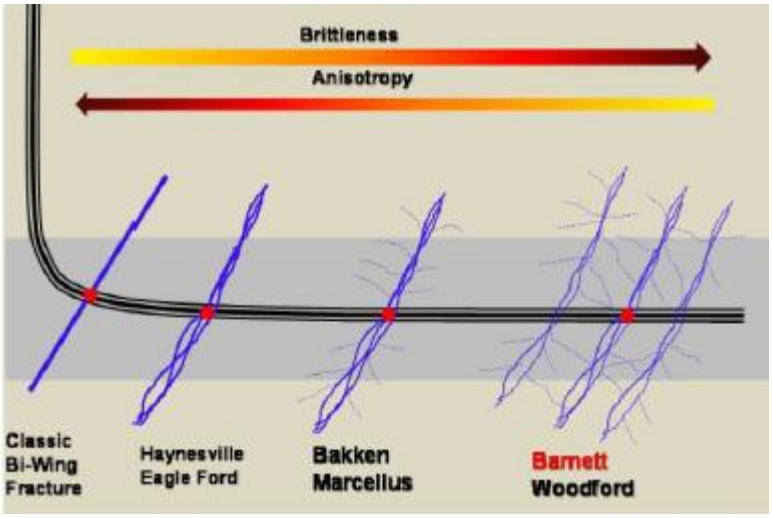

Figure 27. Fracture shape based on different rock fabric and stress anisotropy (Najed et al. 2013)

Rather than multi-stage fracture, single stage fracture was used in order to save computational time and resources. **Table 1** summarized the reservoir parameters used for the simulation. The perforation depth is at 8600 ft. where the lateral wellbore is placed (center of pay zone). The stress and permeability profile is shown in **Figure 28**. 3D Fracture model is exploited with lumped-parameter leak off model and fracture orientation is vertical with the assumption that vertical stress is higher than horizontal stress at this depth. **Table 2** summarized the materials in fracturing design. Fracturing fluid is cross-linked gel with 50 lb/Mgal loading and 2% KCl resulting in an apparent viscosity of 231.2 cp, wall building coefficient of 2.04×10^{-3} ft. /$\text{min}^{1/2}$, and spurt loss of 0.00774 gal/ft^2. Hence, proppant transport model is convection. Sand proppant is 40/70 Brady sand having specific gravity of 2.63 and diameter of 0.010 in. Ceramic proppant is 40/70 CarboProp (IDC) having specific gravity of 3.28 and diameter of 0.012 in. For resin coated sand, 40/70 curable resin coated sand is used which has a specific gravity and diameter of 2.55 and 0.015 in, respectively. Also, conductivity or permeability measurement (Baseline conductivity) of this RCS is performed at 250 °F which equal to

reservoir temperature so this measurement is applicable to use in the model (Properties of resin change at different temperature). This fracturing design is based on a pump rate at 20 bbl/min and slow proppant concentration ramping rate. An example of a treatment schedule is shown in **Figure 29** including pad, slurry, and flush stages. In order to achieve optimal fracturing design, fracture length and proppant concentrations were altered as shown in **Table 3.** Fracture conductivity and height in each section of fracture from wellbore to tip are investigated as shown in **Figure 30** with association of gelling damage, proppant embedment, and proppant transport (convection) effect that are offered in-house. Also**,** fracture conductivity obtained from this model is used as input for the reservoir simulation model (Chapter 3).

Table 1. Reservoir description for Niobrara tight oil

Parameter	Value	Unit
Reservoir pressure	6500	psi
Reservoir temperature	250	°F
Pay zone depth	8450	ft.
Pay zone thickness	300	ft.
Reservoir permeability	0.000125	mD
Reservoir porosity	0.065	
Bubble point pressure	2500	psi

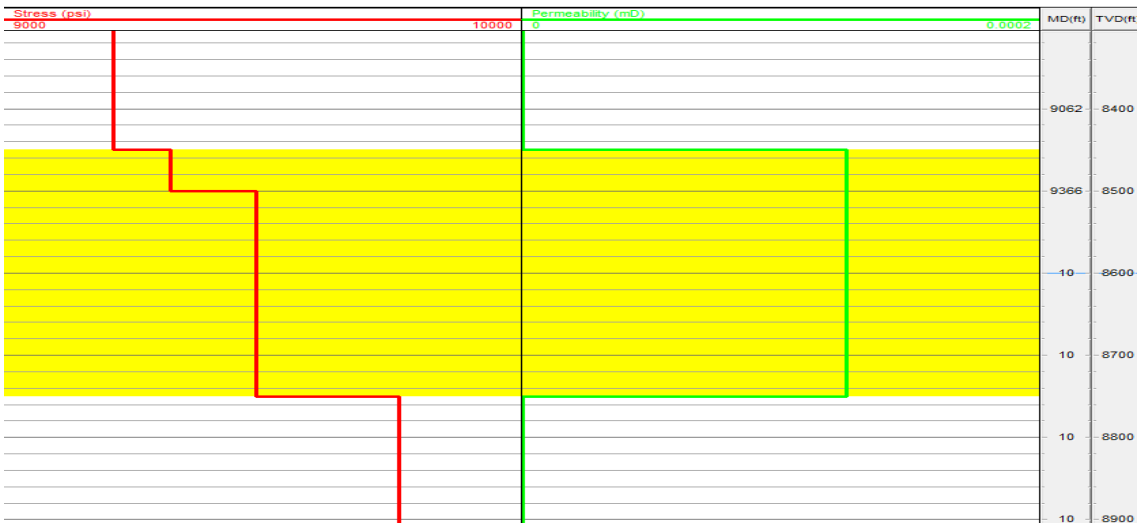

Figure 28. Stress and permeability profile of pay zone (Yellow label)

Table 2. Type of fracturing fluid and proppant in the fracturing design

Materials	Type
Fracturing fluid	Cross-linked
Proppant	1. 40/70 Sand 2. 40/70 Resin-coated sand 3. 40/70 Ceramic

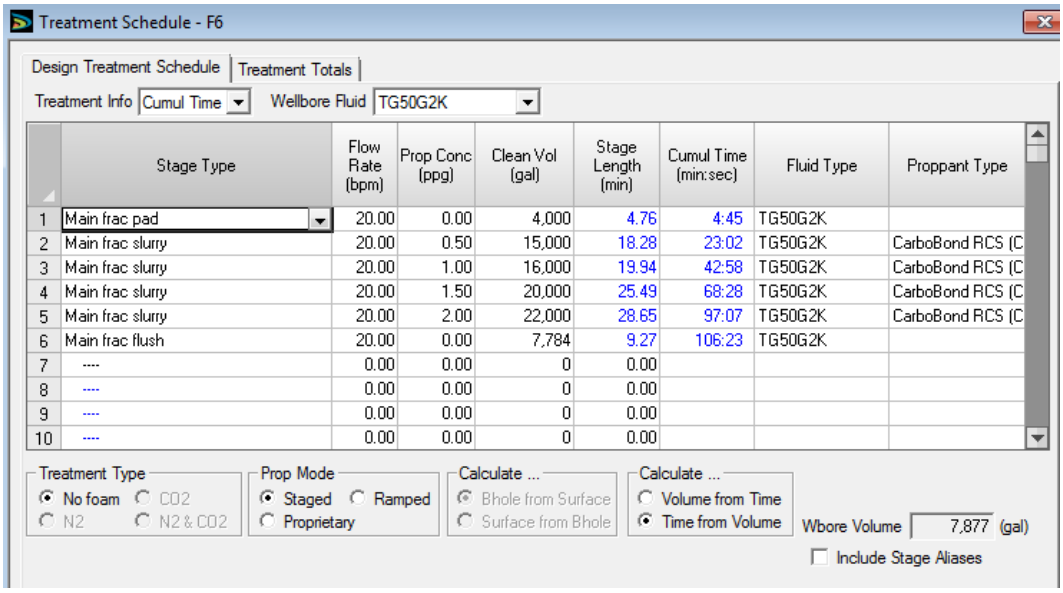

Figure 29. Example of fracturing treatment schedule

Table 3. Range of fracture half-length and average proppant concentration used for optimization

Parameter	Value
Fracture half-length	200-500 ft.
Average proppant concentration	0.02- 0.46 lb/ft^2

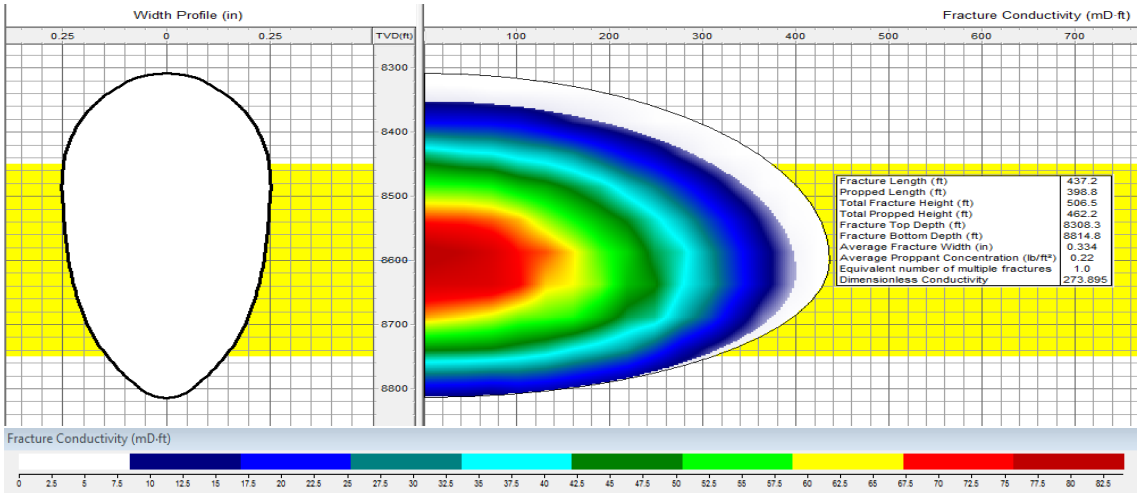

Figure 30. Fracture geometry and conductivity of each fracture zone created by Fracpro

2.2 Modelling Fracture Conductivity Decline

The effect of gelling damage, proppant embedment, and proppant transport (convection) on fracture conductivity are directly obtained from Fracpro. This set of data are acquired from experimental results. In case of gelling damage, I use the value of conductivity loss suggested by the software which equals to 50-70 % for cross-linked fracturing fluid depending on polymer concentration loading as shown in **Figure 31**. (Weaver et al. 2015) introduced a rapid-gel-method to quantify the potential of gel damage on fracture conductivity in the way of reducing assessment cost and time compared to API regained conductivity tests. The regained conductivity due to gel damage for four different fracturing fluid types is shown in **Figure 32**. The range of retained conductivity for fluid A (Conventional borate cross-linked guar-base) is from 35 to 45 %, indicating that the assumption of conductivity loss due to gel residue from Fracpro is reasonable.

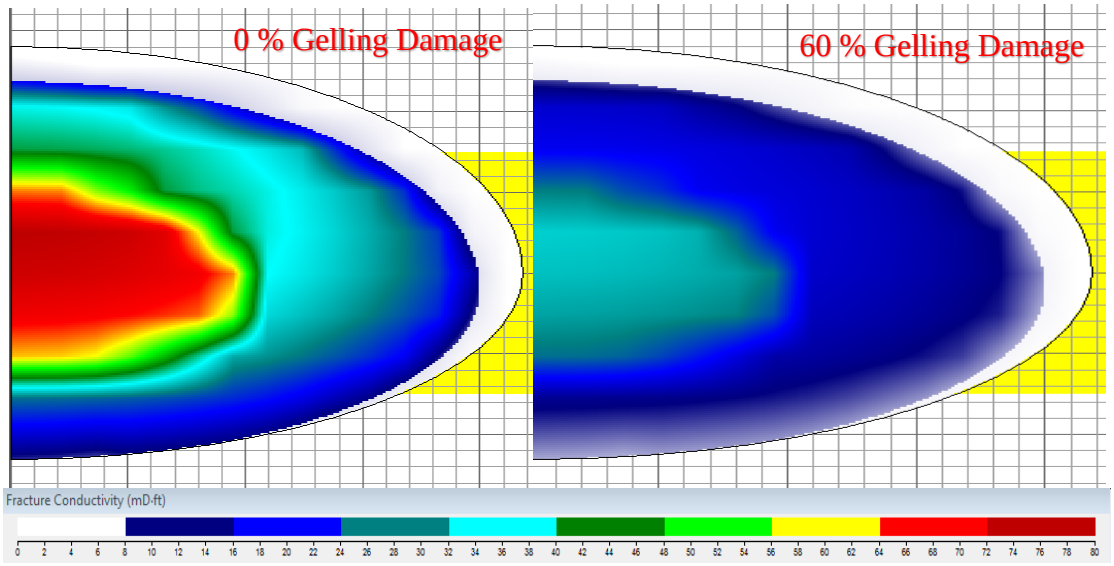

Figure 31. The effect of gelling damage on fracture conductivity

Fluid	Description
A	Borate-crosslinked guar-based (0.3 wt%) fluid with a soluble oxidizing breaker
B	A residue-free, metal-crosslinked, nonguar polysaccharide-based fluid (0.6 wt%) system with an encapsulated oxidizing breaker
C	Borate-crosslinked derivatized-guar-based (0.36 wt%) fluid with a soluble oxidizing breaker
D	Metal-crosslinked, double-derivatized-guar-based (0.36 wt%) fluid with a soluble oxidizing breaker with a catalyst

Table 2—Fluid descriptions.

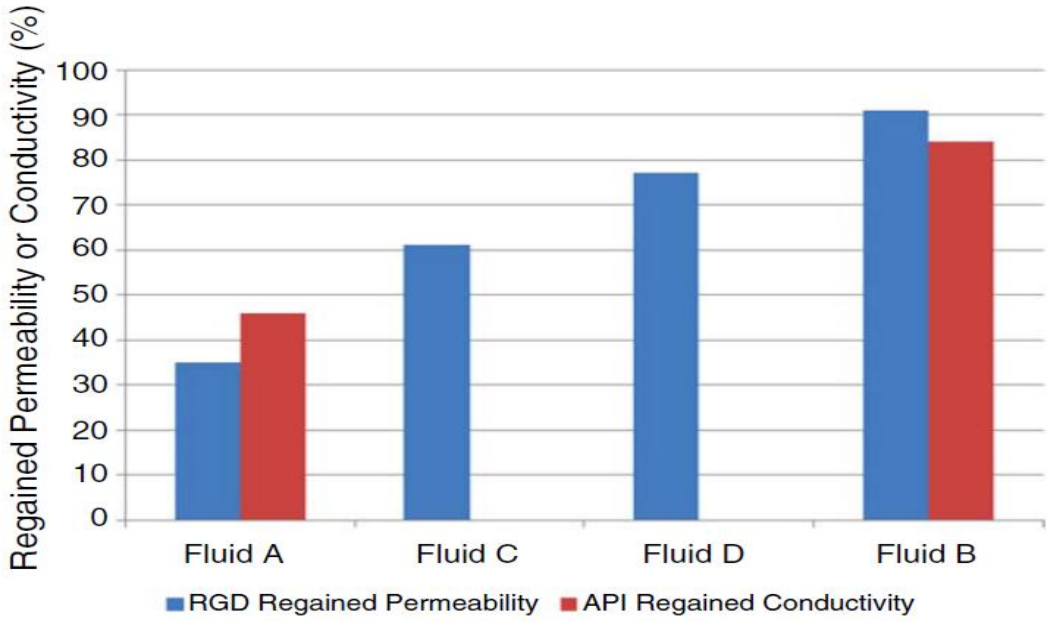

Figure 32. Regained conductivity due to gel damage for four different fracturing fluid (Weaver et al. 2015)

Conductivity loss due to proppant embedment can be achieved directly from Fracpro as shown in **Figure 33**. After inputting depth of proppant embedment value, software will automatically recalculate fracture conductivity after proppant indent into both fracture faces.

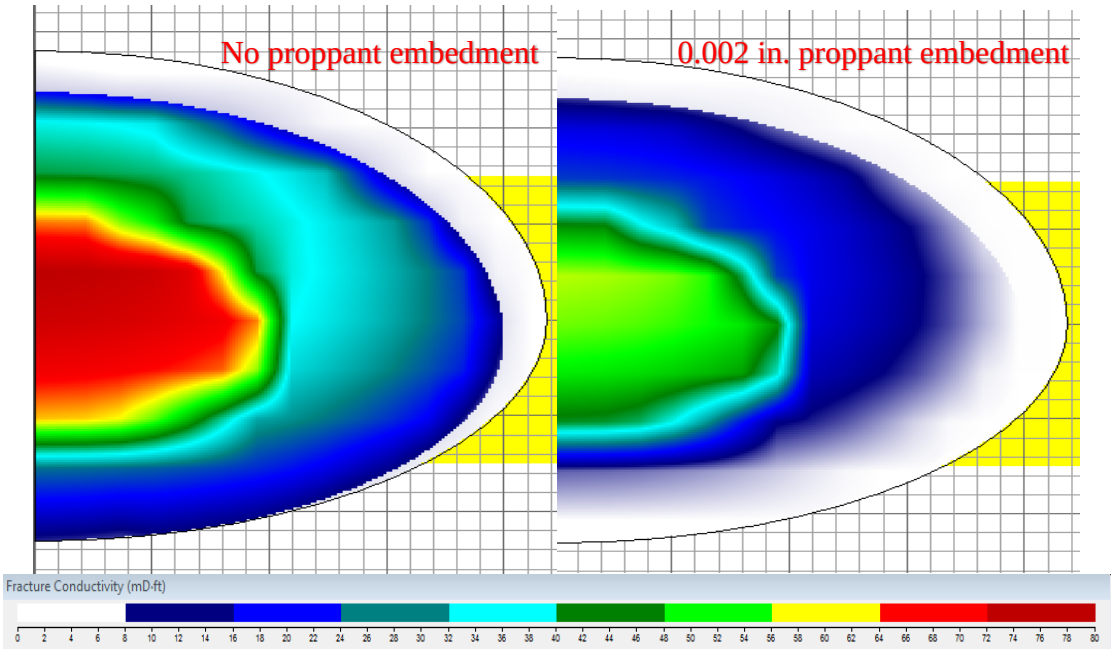

Figure 33. The effect of proppant embedment on fracture conductivity

The depths of proppant embedment are collected from elsewhere. For example, Ghosh et al. (2014) describe the indentation range of 20/40 Ottawa sand can be 30-80 µm at 5000 psi confining pressure and 1000 psi pore pressure for Barnett shale sample. For 30/50 resin-coated sand, indentation ranges from 20-60 µm, which is less than that of Ottawa sand. Indentation of 40/70 Ceramic proppant is deepest ranging from 50-80 µm. Proppant embedment depth is usually a function of stress, rock Young's modulus, and proppant diameter as discussed in Chapter 1. For example, Laboratory-base measurement determined the fracture width reduction due to proppant embedment by **Equation 12** (Palisch et al. 2010).

$$W_E = \frac{2.5 d_P}{\left(1+\frac{4000E}{\sigma}\right)^{1.5}} \qquad (12)$$

Where, W_E is width loss, d_P is proppant diameter, E is Young's modulus of rock (MMpsi), and σ is the closure stress (psi). However, from the literature review, different types of proppant with same proppant diameter exhibit varied proppant embedment depth with

unchanged of type of rock and stress. Hence, **Equation 12** might not be capable of representing different type of proppant. Also, the Young's modulus of the rock after exposure to fracturing fluid are decreased with varied magnitude, so it's hard to precisely identify the value. In this case, terminal value of proppant embedment depth from Ghosh (2014) and other lab measurement are used as an input, and this assumption is reasonable approximation which will be discussed in Chapter 4.

Convection of proppant during suspension in cross-linked fracturing fluid are investigated within Fracpro**.** In this study, three cases of proppant transport can be studied, including best, stratified convection, and worse cases as shown in **Figure 34.** The best and stratified convection cases are based on density difference between the proppant laden stage and entire stage, and these stages move relative to another. The higher density stage tends to sink into bottom of the fracture. For worse case, proppant is assumed to fail completely to suspend in the fluid which all stages are mixed and dropped into bottom of fracture. Moreover, for the best convection case, fracture conductivity near the wellbore is high, but it is low at fracture tip region, so this case can represent the high convection case as mentioned in Chapter 1; where convection leads to lower proppant coverage (lateral) and fracture conductivity in the fracture tip area such as fracture with Nc value less than one. On the other hand, stratified convection cases, proppant distribution is better than the best convection case which represents the low convection scenario such as fracture with Nc values more than one. Hence, these three scenarios can represent uncertainty associated with stress heterogeneity, which leads to non-uniform fracture width during and after stimulation treatment.

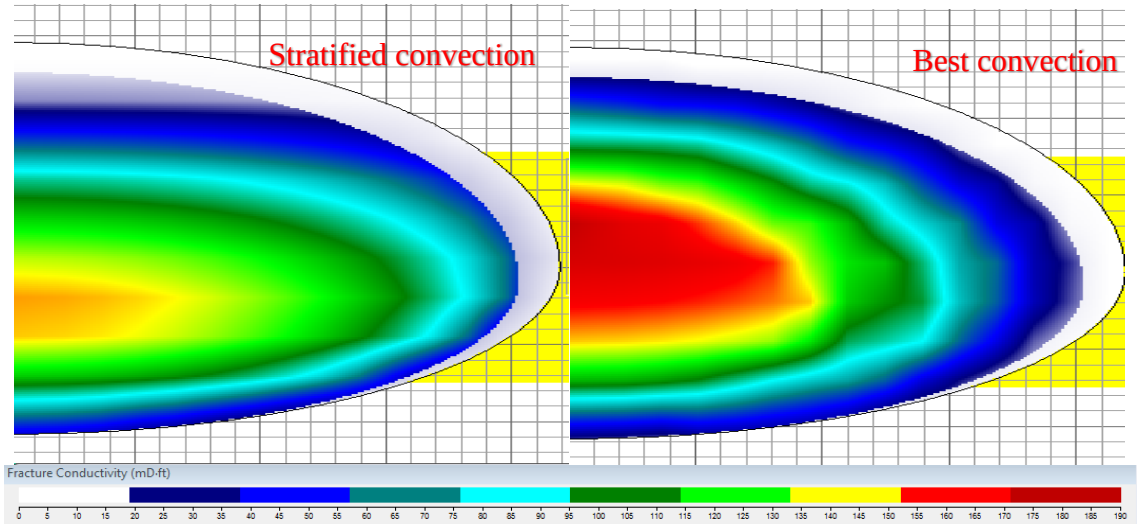

Figure 34. The effect of convection on fracture conductivity

Proppant pack permeability loss (Baseline conductivity) due to crushing of proppant at each confining stress is shown in **Figure 35**. This data is directly acquired from the Fracpro database which are obtained from laboratory results. It is an assumption based on modified API tests (ISO 13503-5), which is conducted at proppant concentration of 2 lb/ft^2. However, in our hydraulic fracture model, proppant concentration is varied from one location to another, and normally less than 1 lb/ft^2. With limitations of data, I assume that proppant crushing of each proppant pack concentration are equal to crushing of proppant pack at proppant concentration of 2 lb/ft^2.

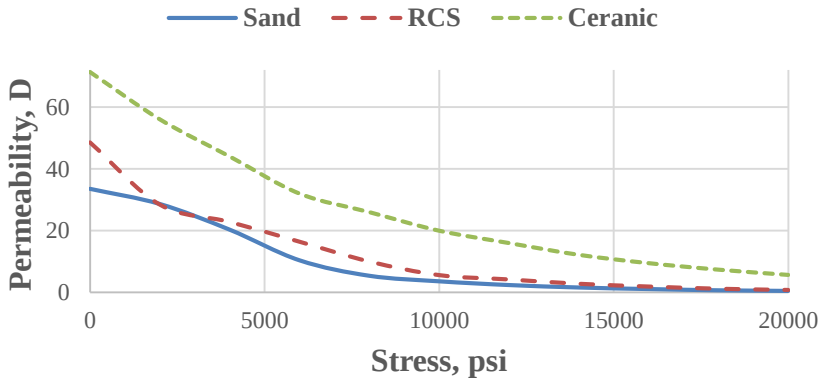

Figure 35. Baseline conductivity for three proppant type

Fine migration and plugging effects on proppant pack permeability are also considered. Ghosh et al. (2014) conducted experiments to determine the permeability change of proppant pack as a function of time as shown in **Figure 36**. The experimental condition is flow rate of 3 ml/min with confining stress of 5000 psi and pore pressure of 1000 psi for a Barnett shale core plug. It shows that sand illustrates a significant permeability drop (99%) in 10 days. Ceramic exhibits 70 % drop in permeability. However, resin-coated sand show no permeability drop during a 10 day period.

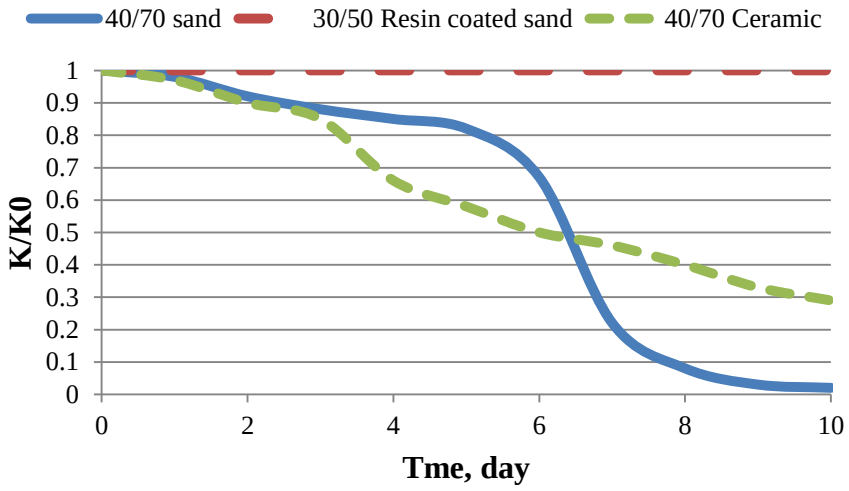

Figure 36. Permeability drop due to fine migration and plugging for each proppant type (Ghosh et al. 2014) (k/ko is ratio of permeability at specific time over initial permeability.) (Experiment procedure and condition are shown in Appendix B1.)

The permeability loss curve due to cyclic stress are collected and derived from experimental data conducted by Schubarth and Milton-Taylor (2004). Author relates median particle diameter (MPD) with fracture conductivity by using Berg's equation (**Equation.10**). **Figure 37** illustrates that conductivity of ceramic proppants strongly relate to MPD. The effect of cyclic stress of different types of proppant were studied as shown in **Figure 38.** Sand experiences higher permeability loss due to stress cycle than

ceramic because it possesses lower crushing strength. For resin coated sand, I cannot acquire data from any literature review, but as we know that resin-coated sand crushes in the same matter with sand, we assume resin-coated sand exhibits similar behavior with sand under a stress cycle.

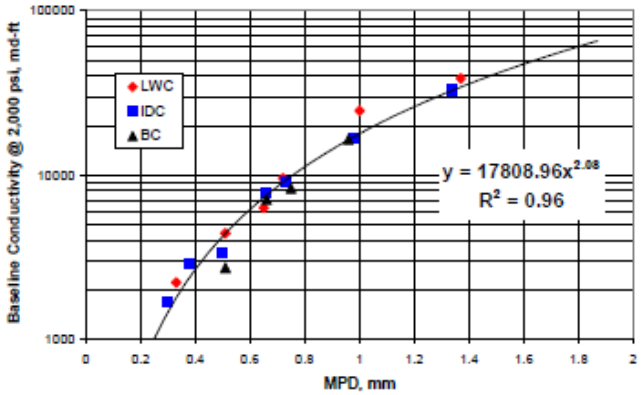

Figure 37. Baseline conductivity versus MPD for ceramic proppant (Schubarth and Milton-Taylor 2004)

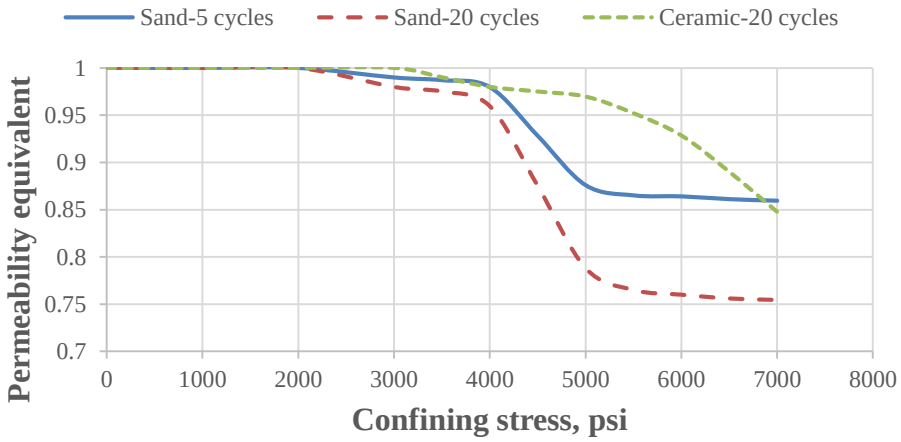

Figure 38. Permeability loss over number of stress cycle for each proppant type (Derived from Schubarth and Milton-Taylor (2004) data) (Experiment procedure and condition are shown in Appendix B2.)

Chapter 3: Reservoir Modeling

A tight oil reservoir model is built to study the effect of conductivity damaging parameters, including gelling damage, proppant embedment and placement, cyclic stress, and fine migration and plugging on well productivity. Also, the economic parameters are incorporated in this model to determine optimal proppant type based on specific conductivity damaging parameters associated for each type of proppant. Finally, optimization of fracturing design is conducted based on economic parameters that will be discussed in later chapter.

In this work, CMG (CMG, 2012) is used to simulate reservoir conditions with a single porosity model. The well has a single hydraulic fracture as mentioned in the previous chapter. The model dimensions are 1550 x 1550 x 300 ft. and the other reservoir properties are shown in **Table 1** in the previous chapter.

3.1 Gridding for Matrix and Hydraulic Fractures

A regular Cartesian grid is used for this model which can be discretized into 31*50 for I direction, 31*50 for J direction, and 1*300 for K direction as shown in **Figure 39.** This model relied on finite difference mathematical approximation, which the accuracy of this approximation depends on grid size. In this study, accurate prediction of fluid flow inside and nearby fracture is paramount. Therefore, a Local Grid Refinements (LGR) technique is exploited to model designed fracture from fracturing model (Chapter 2) and matrix that are close to the fracture. The hydraulic fracture grid is at the finest setting, and grid size is gradually larger as it's far away from hydraulic fracture grid as shown in **Figure 40**. Also, LGR technique helps us to capture transient flow from matrix to fracture (Rubin 2010).

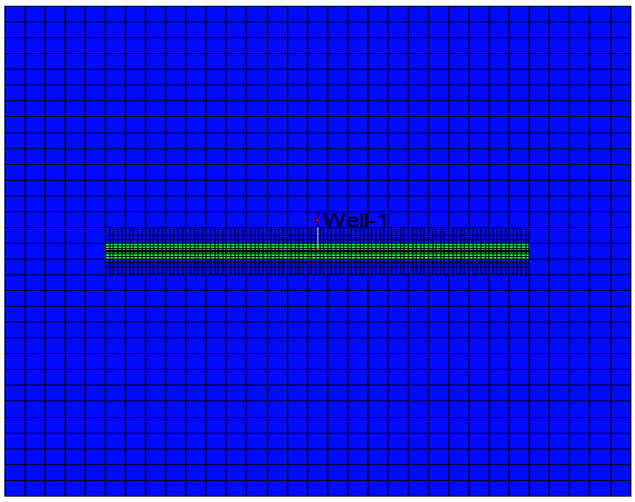

Figure 39. 1550 x 1550 x 300 ft. reservoir model

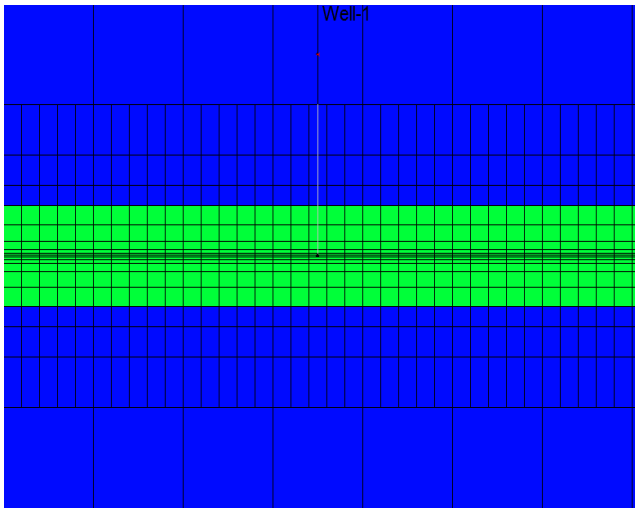

Figure 40. Grid scheme with LGR technique associated

3.2 Permeability Stress Dependence

To simulate hydraulic fracture permeability loss from increased confining stress as shown in **Figure 35**, I use geomechanic modules in CMG (STARS), which relies on plastic and nonlinear elastic deformation model performing finite-element elasto-plastic analysis. The theory of plasticity can be defined as the relationship between stress and strain. When materials undergo elastic deformation, there are two constants used to define stress-strain properties including Young's modulus and Poisson's ratio. To calculate effective stress

as time goes by, simulators require initial in situ stress and Biot's coefficient, then transferring pressure data from reservoir to geomechanic grid is achieved. Pressure inside the fracture decreases in the reservoir grid due to production. Then, this pressure data is sent to the geomechanic grid to calculate effective stress and permeability. Simultaneously, permeability data is transferred to the reservoir grid to calculate production rate for next time step. The initial effective stress is 9500-6500 = 3000 psi as required by the simulator. Biot's coefficient (α) of each proppant can be some value ranging from 0-1 as shown in **Equation 13**.

$$\alpha = 1 - \frac{c_{ma}}{c_b} \tag{13}$$

$$c_b = \frac{3(1-2\upsilon)}{E} \tag{14}$$

Where c_{ma} is matrix compressibility, c_b is bulk compressibility, υ is Poisson ratio, and E is Young's Modulus. If the proppant pack or matrix have high porosity, c_{ma} is significantly smaller than c_b. As a result, the Biot's coefficient (α) will be close to 1 (Abass et al. 2009). Normally, proppant pack has very high porosity so Biot's coefficient is assumed to be 1 in this model.

3.3 Hydraulic Fracture Model

The hydraulic fracture in this reservoir model is varied in half fracture length (200-500 ft.) with 1 foot of fracture width. However, the value of fracture width is not pragmatic due to the fact that real fracture width cannot be 1 foot, so I use fracture conductivity as an input for permeability of fracture in order to make width correction. It will be illustrated in following example. Fracture with permeability of 60 md and 1 foot wide has the same fracture conductivity with 0.2" with fracture permeability of 3600 md. Hence,

fracture conductivity in this case is 60 md-ft., which can easily transfer to permeability of the fracture that has 1 foot width.

Also, each of fracture wing is divided into 10 sections and the purpose is to input different fracture conductivities that are obtain from the hydraulic fracturing model (Chapter 2) as shown in **Figure 41**. The advantage of using the fracturing (Chapter 2) model compared to a uniformed fracture conductivity model is that a non-uniformed fracture conductivity model is a better representative of a hydraulic fracture created when a ramp up in proppant concentration is frequently used to maximize amount of proppant, which can be injected into fracture while decreasing potential screen-outs. Hence, fracture conductivity is highest at near wellbore region, while fracture conductivity at the tip of fracture is lowest as shown in **Figure 41**. Comparison of reservoir pressure distribution after 15 years of production between non-uniformed and uniformed fracture conductivity models are shown in **Figure 42**. To make them comparable, fracture conductivity of uniformed fracture conductivity model is an average of fracture conductivity from non-uniformed fracture conductivity model. Reservoir pressure distribution is different for both models where cumulative production is also expected to be obviously disputed as shown in **Figure 43**.

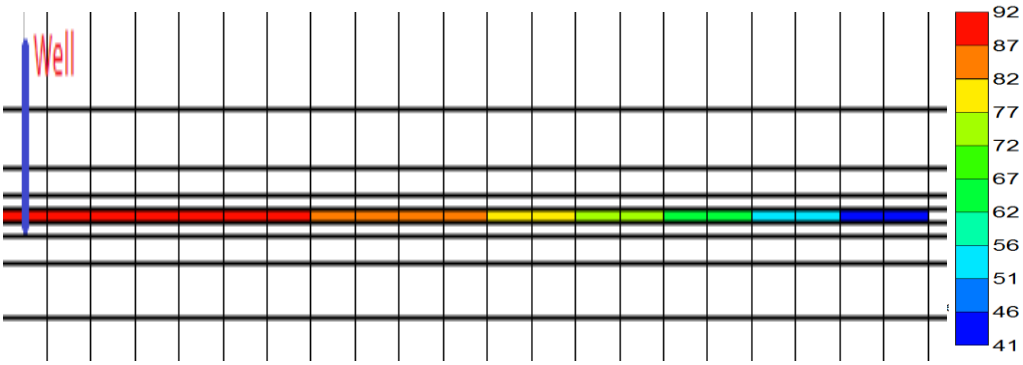

Figure 41. Fracture conductivity (mD-ft.) of each fracture section.

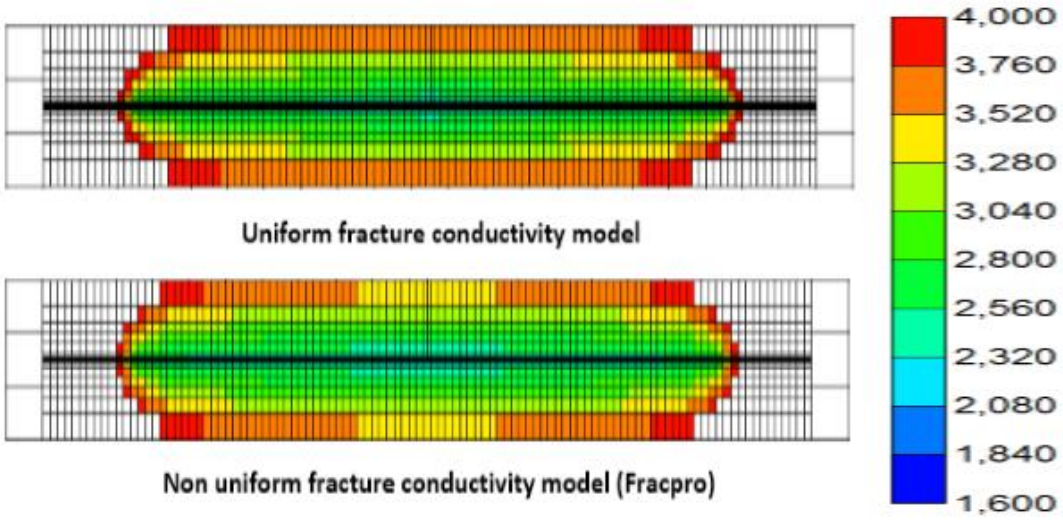

Figure 42. Pressure distribution after 15 years of production for different fracture models (psi)

3.4 Main Assumption for Model Construction

Both mathematical and physical approximation in this model cannot exactly reproduce all the phenomena that occur in the reservoir. Due to insufficient data and complication of simulation, some assumptions of physical phenomena are necessary to apply into a mathematical model which is expected to generate similar behavior for both hydraulic fracture and reservoir. The following are the main assumptions used to construct the simulation model.

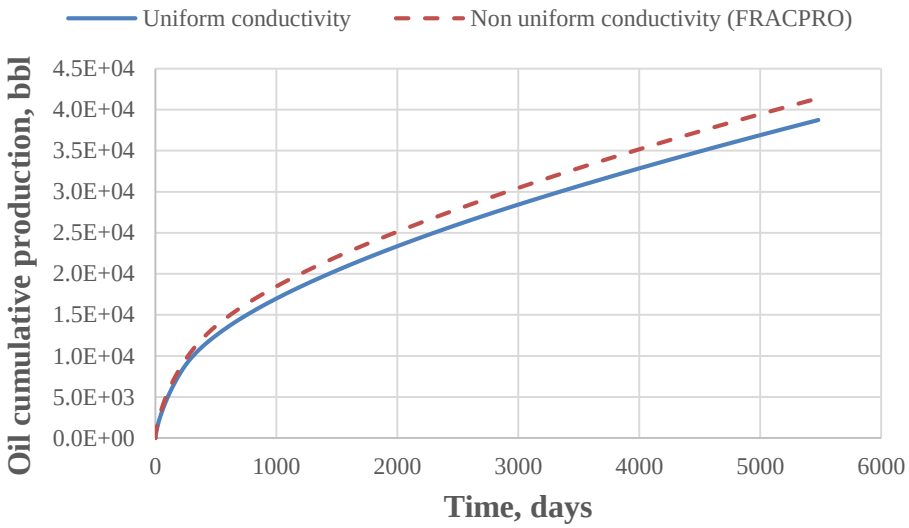

Figure 43. Cumulative oil production for 15 years of different fracture models

Hydraulic fracture is modeled as a bilinear fracture. Even though I use high viscosity fracturing fluid incorporated with very low permeability formation (nano-scale), which can significantly reduce fluid leak off. Also, I assume the formation behave in a ductile manner, which can reduce the complexity of fracture. This fracture configuration is difficult to find after stimulation treatment because fractures prefer to grow in the direction of weakness plane, much like a natural fracture which is not considered in this model. Also, simulated reservoir volume (SRV) is not included because SRV is considered very low when high viscosity fracturing fluid (low leak off coefficient) is used. Also, SRV is difficult to predict. However, this assumption is sufficient to duplicate fracture geometry for cross-linked fracturing fluid system with nano-scale permeability formation.

Fracture permeability loss curve due to either proppant crushing and cyclic stress are products of experimental data based on proppant pack with proppant concentration of 2 lb/ft^2. In fact, the decline conductivity curve of fracture can be varied depending on

proppant concentration (Palisch et al. 2009) because different concentrations of proppant will alter the degree of proppant crushing. However, future research on this subject is necessary to conduct and combine into studied model.

In this study, each conductivity damaging parameters are independent of each other. It means that the result of one damaging parameter has no effect on other damaging parameters. For example, gelling damage effect has no impact on the degree of fine migration and cyclic stress. However, in reality, gelling damage can alter pore structure inside proppant pack, which decreases pore throat size. As a result, fine migration and plugging will be different from the case without gelling damage. Further explanation is mentioned in Chapter1.

The hydraulic fracture model in this study is assumed to be smooth a face while real fracture face tends to be rough. Rough face fracture is expected to alter both proppant crushing value and proppant transport (Palisch et al. 2010). Proppant placement is not evenly distributed in rough fracture face as shown in **Figure 44**. As a result of uneven proppant distribution, the proppant layer is varied from one place to another that can significant change degree of proppant crushing because of difference in stress distribution. However, this overpower the capacity of a fracturing simulator and further research is needed to satisfy real fracture condition.

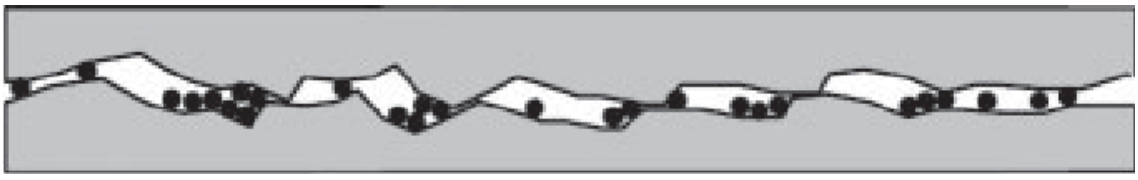

Figure 44. Fracture face scheme from laboratory testing (Palisch et al. 2010)

Chapter 4: Results and Discussion

In this study, effects of each damaging parameter on well productivity is investigated. The bottom hole pressure is constant at 2,600 psi, which is higher than the bubble point pressure (2,500 psi), so I expected to produce only oil at reservoir conditions. For sake of simplicity, I created one hydraulic fracture scenario where all the parameters are shown in **Table 4.**

Table 4. Fracture description for studying the effect of damaging parameters on well productivity

Parameter	Value	Unit
Half fracture length	400	ft.
Proppant type	40/70 Sand	
Proppant concentration	0.02	lb/ft^2

The behavior of fracture pressure and conductivity as a function of time is shown in **Figure 45,** illustrating that fracture pressure reduces vastly in a very short period of time after production starts because of significant difference between fracture and matrix permeability. This difference allows a rapid increased net confining stress and fracture conductivity drop. (Quintero and Devegowda 2015) investigated choke management in shale wells for mitigated rapid fracture conductivity loss which can promote fracture conductivity retention. He concluded that choke management cannot alleviate this effect, and the optimal strategies is the largest choke setting because of a higher initial productivity index, and NPV. Obviously, damaging parameters such as proppant crushing, embedment, cyclic stress, and fine plugging are expected to affect well productivity from the very early life of production when largest the choke setting is applied.

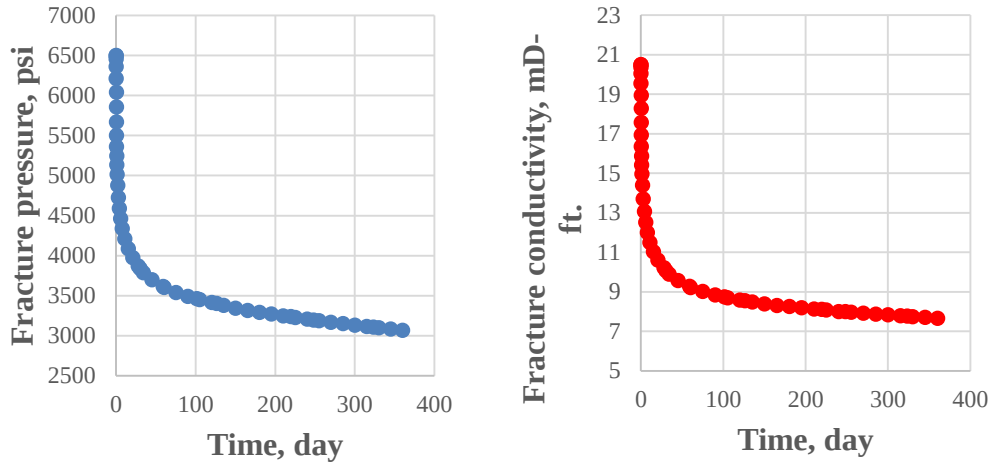

Figure 45. Pressure inside fracture and fracture conductivity as a function of time

4.1 Effect of Conductivity Damaging Parameters

4.1.1 Gelling Damage

In our model, cross-linked fluid is used for both fracturing and proppant laden stages. The degree of damage ranges normally from 50 to 70 %, depending on the concentration of the loading polymer, breaker type, etc. Well performance with and without gelling damage is shown in **Figure 46.** In our model, the gel residue equally damages conductivity for each section of fracture. Gelling damage effect is more important at early stages of production life (first year). Cumulative production is reduced by 10-16 % due to conductivity loss by gel residue over 15 years.

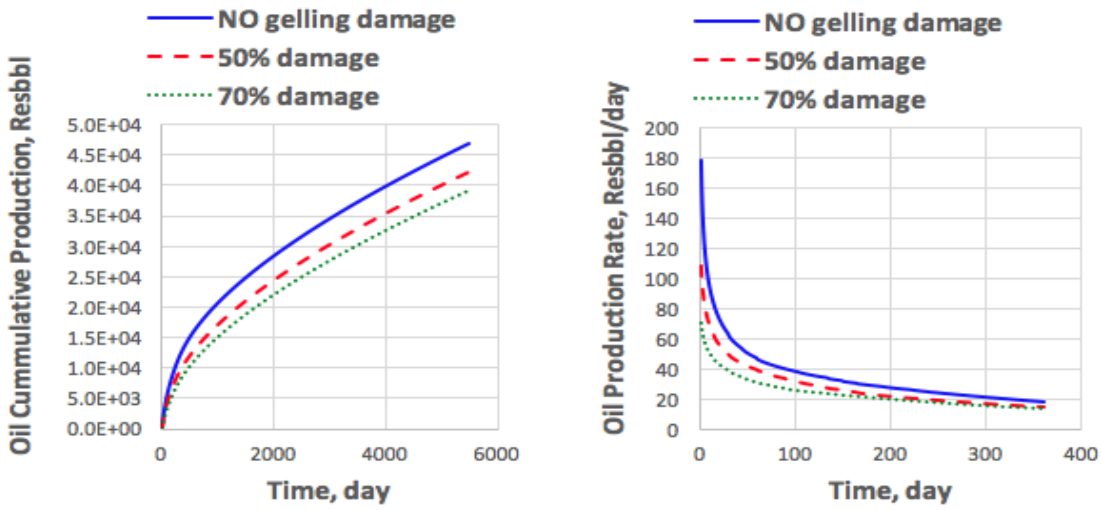

(a) Oil cumulative production over 15 year (b) Oil production rate over 1 year

Figure 46. Effect of gelling damage on well productivity

4.1.2 Proppant Embedment

Indentation of proppant is one of uncertainty in hydraulic fracturing. Due to reservoir heterogeneity, such as differences in rock composition that can alter Young's modulus or stress distribution in the vicinity of hydraulic fracture, embedment of proppant can be varied (Denney 2012) and (Zhang et al. 2015). In this study, the degree of indentation ranges from 0.000-0.003 in. Cumulative production and production rates are illustrated in **Figure 47**. Obviously, the difference in well performance between 0.000 and 0.001 in. embedment scenarios are considerable; while differences in cumulative production for 0.001 and 0.002 in. indentation are not as significant. The reason is, with a small degree of proppant embedment, conductivity of fracture in fracture tip regions are significantly reduced due to them containing very low proppant concentration (smaller width when compare with near wellbore region). However, indentation of proppant can affect well productivity throughout the production life, and can notably diminish cumulative production by 25-52 % after 15 years of production.

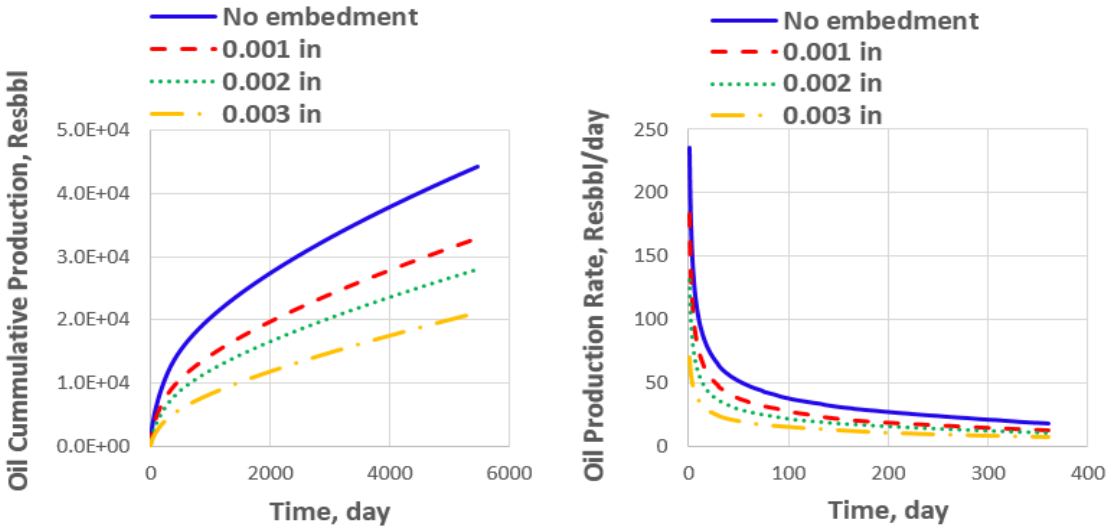

(a) Oil cumulative production over 15 year (b) Oil production rate over 1 year

Figure 47. Effect of proppant embedment on well productivity

4.1.3 Proppant Placement and Transport

In this model, cross-linked fluid is used to deliver proppant in the fracture. Therefore, convection is more important than particle settling in this situation. Proppant concentration at the fracture tip can be lessened by convection effects due to particles accumulated in or near the wellbore region of the fracture, as shown in **Figure 34.** As a result, fracture conductivity near the tip region is significantly lower than near the wellbore region. Cumulative production and production rates are shown in **Figure 48.** Convection effects seem not be important at early stages of production, but start to influence cumulative production after 3 years of production. Hence, proppant placement is more important for long term well productivity.

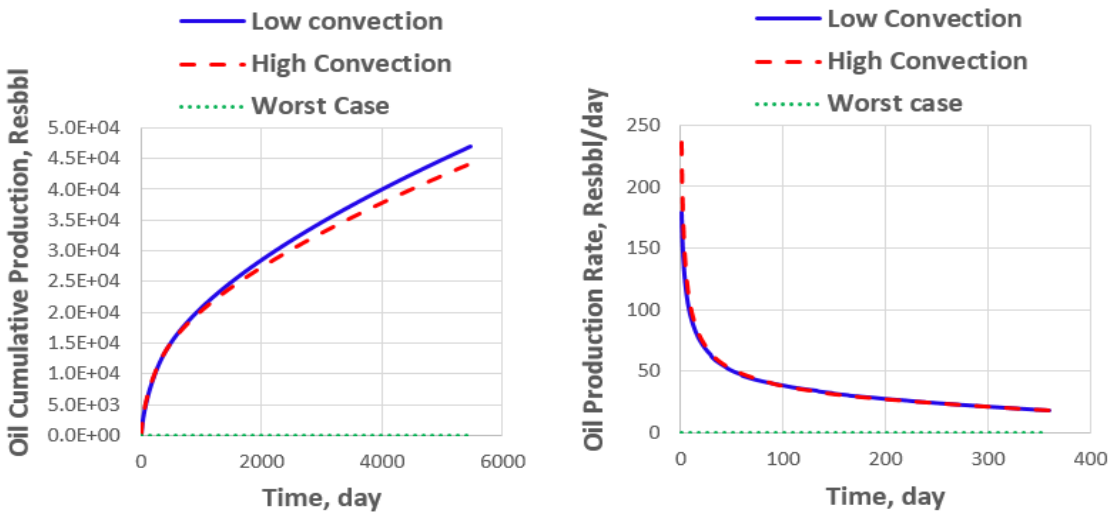

(a) Oil cumulative production over 15 year (b) Oil production rate over 1 year

Figure 48. Effect of proppant placement (convection) on well productivity

In addition, I also incorporate the unsuccessful proppant placement scenario (worst case) due to faulty design. In this scenario, proppants sink to bottom of the fracture, which most of the area is not in the pay zone. From **Figure 48,** cumulative production is considerably lower than other cases, and such epidemic scenarios sometimes occur in the field by design flaw. However, this effect is not detrimental in higher proppant concentration fractures because the fracture can still be propped by some of the proppant due to a higher amount of proppant injected. Therefore, proppant placement is one of the most important parameters we need to consider to achieve successful hydraulic fracturing.

4.1.4 Cyclic Stress

Temporary shut-in and start production is unpredictable depending on many factors such as market demand, well maintenance, etc. In this model, we simulate 3 cases including 1 (base case), 5, and 20 stress cycles, as it matches acquired experimental data. Impacts of

cyclic stress on cumulative production and production rates are shown in **Figure 49**. In this case, the cyclic stress effect on production decreases cumulative production by 4-6 % over 15 years, and cyclic stress is deemed insignificance in this scenario.

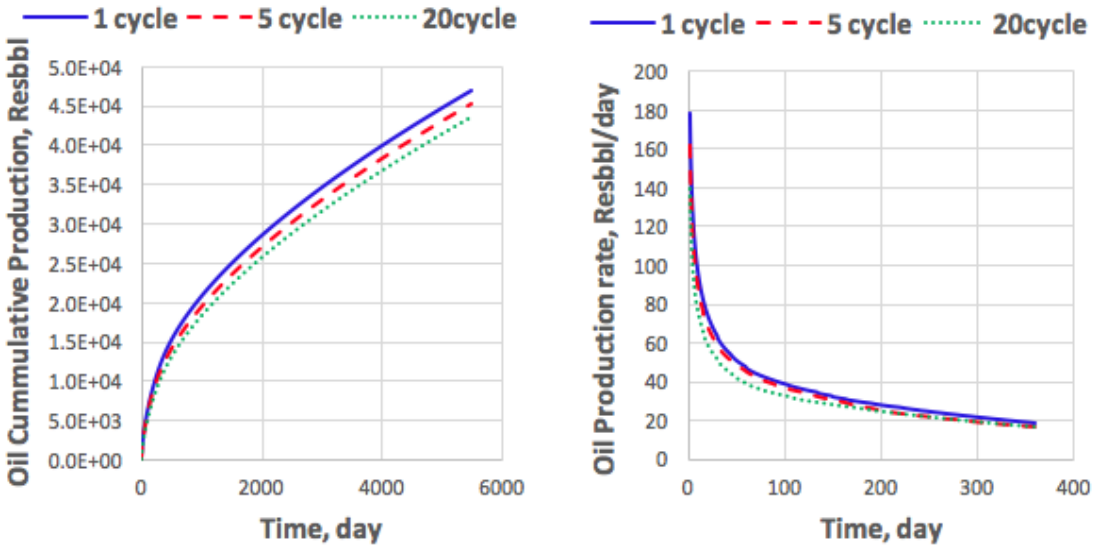

(a) Oil cumulative production over 15 year (b) Oil production rate over 1 year

Figure 49. Effect of cyclic stress on well productivity

4.1.5 Fine Migration and Plugging

In this model, sand is used as a proppant which can generate plenty of fine particle under confining stress. Those fines tend to migrate and plug pore space which significantly reduces proppant packing permeability by 99 %. Impacts of fine plugging on well productivity is shown in **Figure 50.** It shows that plugging pore space illustrates tremendous impact on cumulative production and production rates from the beginning to the end of the production life (15 years). Cumulative production declines by 44 %. Obviously, the negative effect is more pronounced at the early time of production.

However, the fine plugging effect is not deleterious when resin coated sand or ceramic are used as proppant.

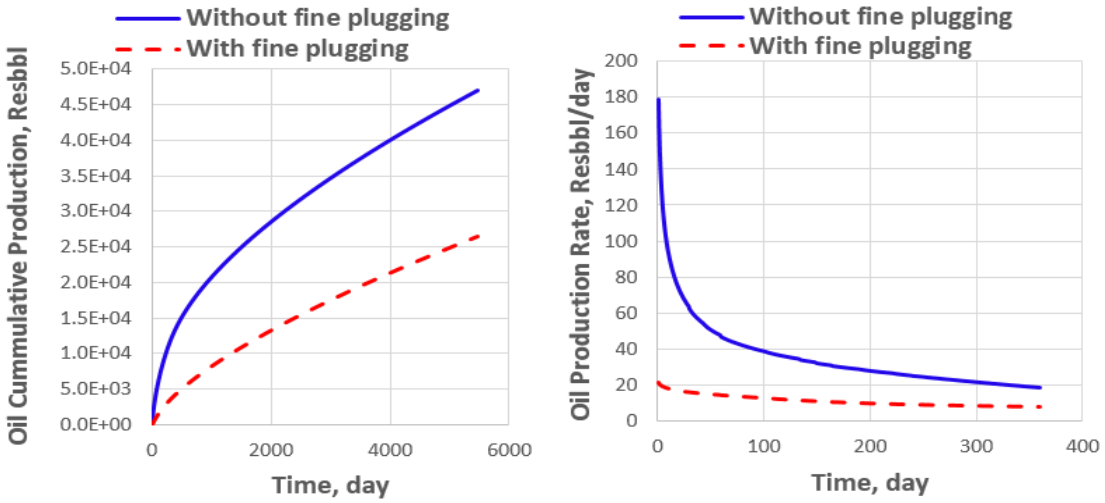

(a) Oil cumulative production over 15 year (b) Oil production rate over 1 year

Figure 50. Effect of fine plugging on well productivity

4.1.6 Combination of Damaging Parameter

In order to achieve precise well productivity for hydraulic fractured wells, all of the damage parameters must be included in the simulation model. **Table** 5 illustrates the degree of damaging parameters.

Table 5. Degree of damaging parameters

Damaging Parameter	Value	unit
Gelling damage	60 %	
Proppant indentation	0.002	in.
Proppant convection	High	
Stress cycle	5	cycle

Also, fine plugging effects inevitably incorporates into this model because it seems to have the highest impact on productivity. Impact of damaging parameters on cumulative production and production rates are shown in **Figure 51.** Cumulative production is

reduced by 46 % corresponding to all damage excepted fine plugging. A 73 % reduction of cumulative production is presented when fine plugging is included. Moreover, the initial production rate can be totally different from non-damaged and damaged cases (178.46 to 7.65 Resbbl/day). Hence, without integration of damaging parameters into fracture simulation, prediction of well performance is far more incorrect. Also, reservoir pressure distribution is totally different for both cases as shown in **Figure 52**.

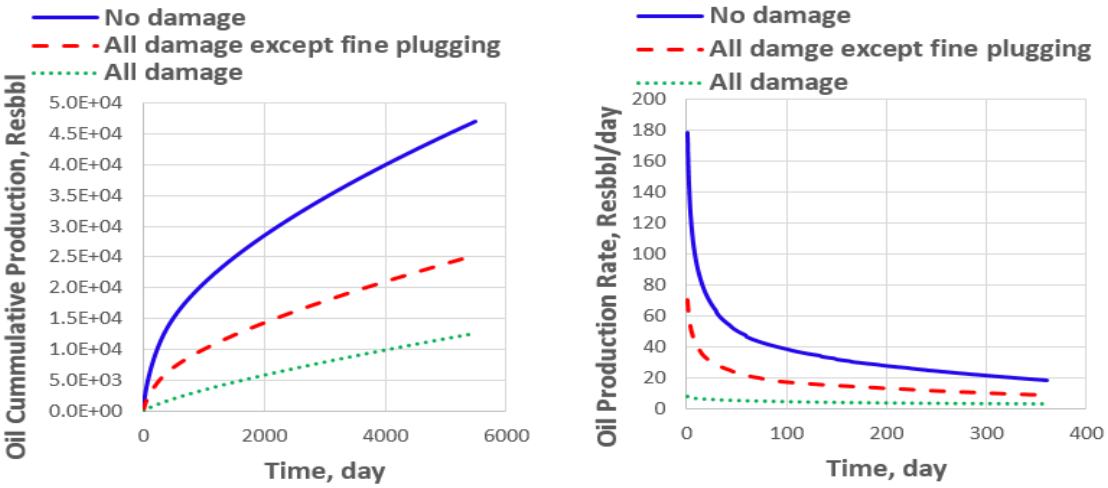

(a) Oil cumulative production over 15 year (b) Oil production rate over 1 year

Figure 51. Effect of combined damaging parameters on well productivity

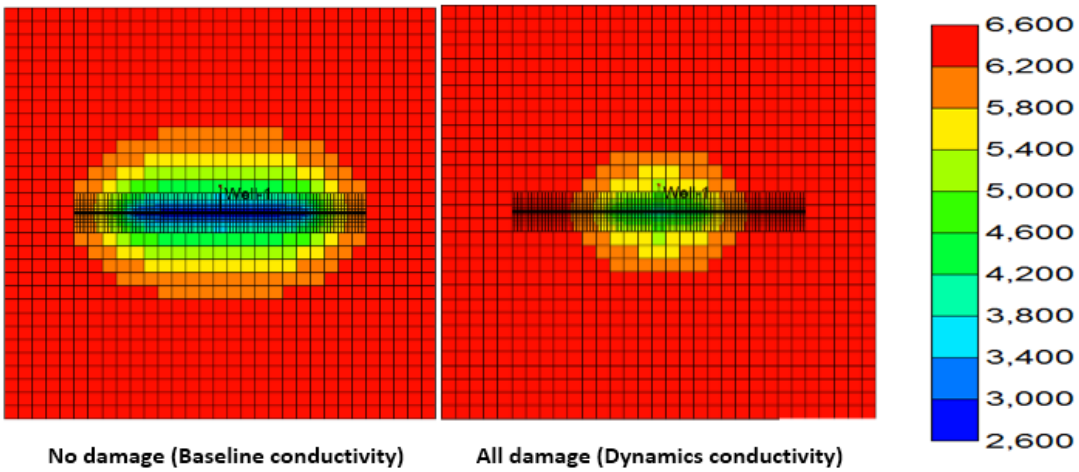

Figure 52. Pressure distribution after 15 years of production (psi)

4.2 Sensitivity Study

In unconventional reservoirs, uncertainty such as degree of reservoir heterogeneity, which can alter degree of damaging parameter is one of its characteristics. For example, clay composition in a shale formation dictates the degree of proppant indentation (Alramahi and Sundberg 2012). Stress heterogeneity can lead to non-uniform fracture which placement (convection) of proppant prediction is unsure (Clark 2006). Moreover, hydraulic fracturing itself is uncertain. In some cases, gelling damage can be very high due to incorporation of fracture complexity, making fracture clean-up highly difficult. Obviously, a number of temporary shut-in or start productions are unknown, so it is hard to predict the stress cycle effect. In this work, we investigate the effect of uncertainties of damaging parameters on well performance for two scenarios. First, low proppant concentration fracture scenario represents attempts to achieve partial monolayer of proppant pack, or to reduce fracturing cost. Fracture with intermediate proppant concentration illustrates the second scenario. I expected that the effect of damaging parameters on well productivity are varied and depended on proppant concentration (fracture width). Four uncertainty parameters, including gelling damage, proppant embedment, proppant placement, and cyclic stress are examined to quantify the critical parameter. Reasonable range of each damaging parameter are given in **Table 6**. However, fine migration and the plugging effect is included in the simulation, but it does not represent sensitivity analysis due to the limited data we can acquire.

Table 6. Four damaging parameters used for sensitivity analysis

Symbol	Parameter	Minimum value	Maximum value	Unit
Gelling damage	A	50 %	70 %	
Proppant Embedment	B	0.000	0.002	In.
Proppant placement	C	Low convection	High convection	
Cyclic stress	D	5	20	Cycle

To perform sensitivity analysis, I adopt Design of Experiment (DOE) technique (Minitab 17) to investigate the effect of changing degree of the damaging parameters on well productivity. Experimental design technique is a set of experiments aimed to describe, or explain the effect of uncertainty of controllable and uncontrollable factors on output. Controllable factors can be something that an experimenter can control, such as bottom hole pressure while uncontrollable factors are factors that are impossible to change, such as porosity or fluid saturation (Collins et al. 2015). This technique is very versatile and very useful. For example, optimization of the process can be done with an unknown influence of number of parameters, or a screening experiment might be used to investigate the influence on the response. In fact, there are plenty of other design approaches including fractional factorial design, surface design, and etc. In this study, we employ a two level fractional factorial design. Two level means that minimum and maximum value of each factor are used, so the number of runs to complete analysis with every combination is 2^n, where n is number of factors. For this study including 4 factors, number of runs should be 16, but the resolution can be adjusted to reduce number of runs. Rather than using full factorial design (16 runs), half factorial design (8 runs) is a reasonable design to characterize the uncertainty of damaging parameters on well productivity. The benefit of utilizing this method is the reduction of computation time without a loss of captured effect. This effect can be classified into two categories: single and interaction (interaction of two or more damaging parameter) effect. 8 cases based on two-level fractional factorial are created according to four damaging uncertainty parameters as shown in **Table 7**. Also, we divide sensitivity analysis into 2 periods: 7 and 15 years.

Table 7. 8 different cases based on two level fractional factorial design (-1 is minimum value and 1 is maximum value)

Run cases	Damaging parameter			
	A	B	C	D
1	-1	-1	-1	-1
2	1	-1	-1	1
3	-1	1	-1	1
4	1	1	-1	-1
5	-1	-1	1	1
6	1	-1	1	-1
7	-1	1	1	-1
8	1	1	1	1

4.2.1 First Scenario: Low Proppant Concentration

Cumulative production for these 8 cases range from 247.0 to 18755.41 resbbl after 15 years of production, shown in **Figure 53**. Huge differences between the minimum and maximum number can be captured by experimental design method as shown in **Figure 54**, illustrating that ranking from the most to least important parameter is proppant embedment, proppant placement, interaction between proppant embedment and placement, gelling damage, then cyclic stress. This sensitivity analysis leads to answer why one of our cases has cumulative production at only 247.03 resbbl. In that case, 0.002 in proppant indentation and low convection are associated into the model, determine that uniformly distributed proppant in the fracture (low fracture width), and fracture width is greatly reduced by proppant embedment effect. The above explanation confirms this sensitivity analysis that the top three important parameters are proppant embedment, proppant placement, and interaction between proppant embedment and placement. The rank of critical parameters are the same for both 7 and 15-year periods.

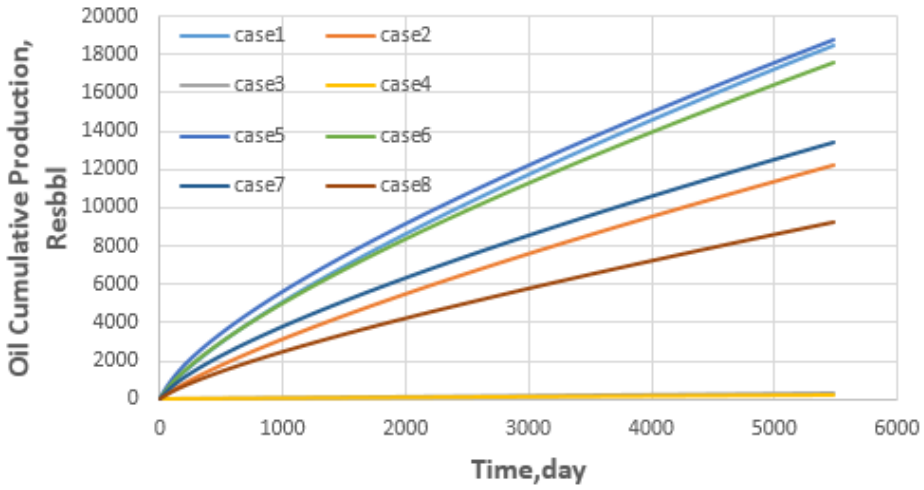

Figure 53. Oil cumulative production of 8 difference cases

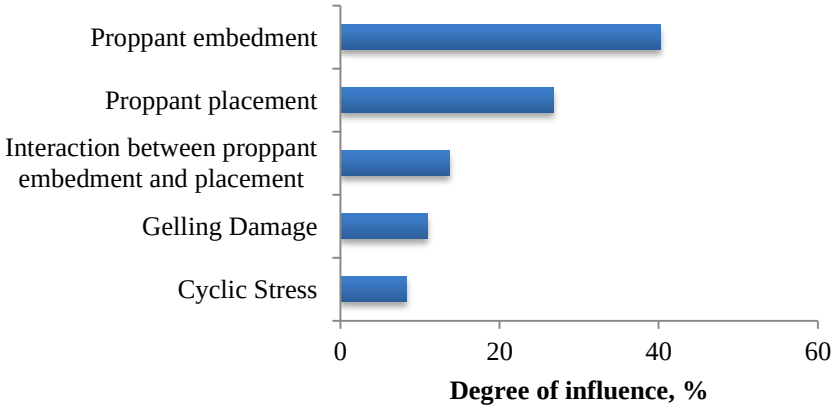

(a) Short-term (7 years)

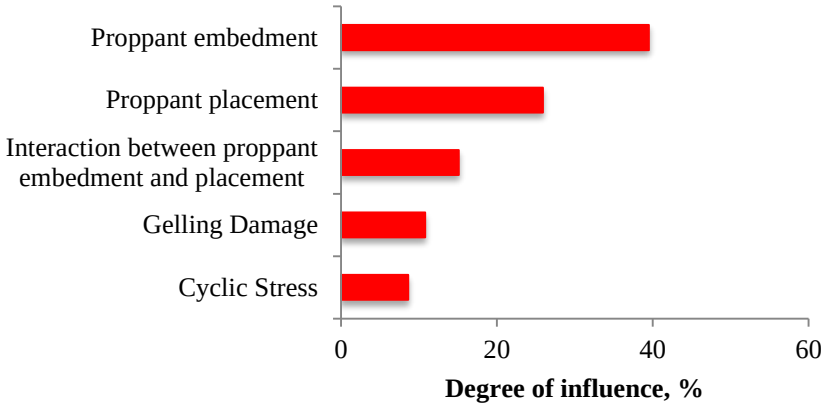

(b) Long-term (15 years)

Figure 54. Rank of critical parameters on well performance

4.2.2 Second Scenario: Intermediate Proppant Concentration

Cumulative productions for 8 cases after 15 years of production are shown in **Figure 55** ranging from 25656.4 to 36449.6 resbbl. According to the sensitivity analysis, the ranked degree of influence for 7 and 15-year period are shown in **Figure 56**. For this scenario, gelling damage and cyclic stress seem to be more important to well productivity than proppant embedment, placement, and interaction between those two effects for both 7 and 15 year periods. The reason might be higher proppant concentration than previous scenarios that represents larger fracture width, so proppant embedment and placement has less effect on fracture conductivity reduction.

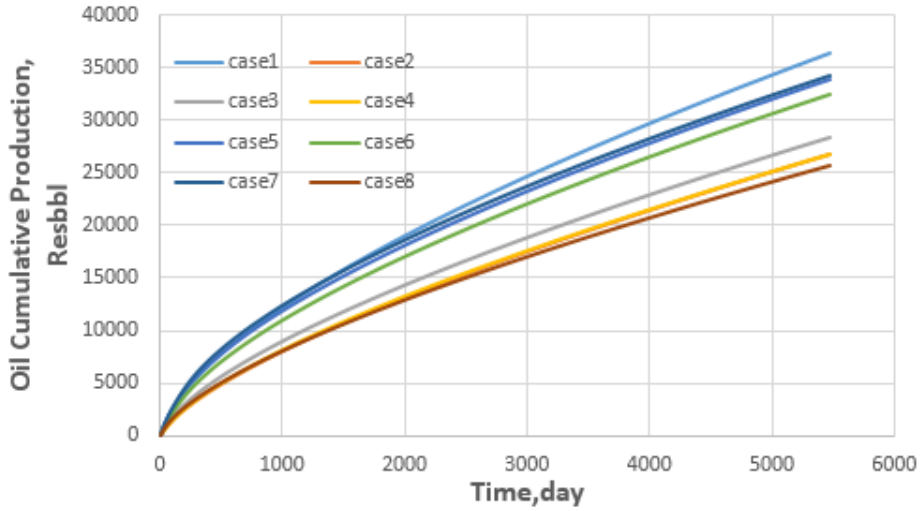

Figure 55. Oil cumulative production of 8 difference cases

Hence, it can be concluded that fracturing design with low proppant concentration should be avoided for a reservoir or proppant type such as soft rock or ceramic proppant, which a high degree of proppant indention is expected.

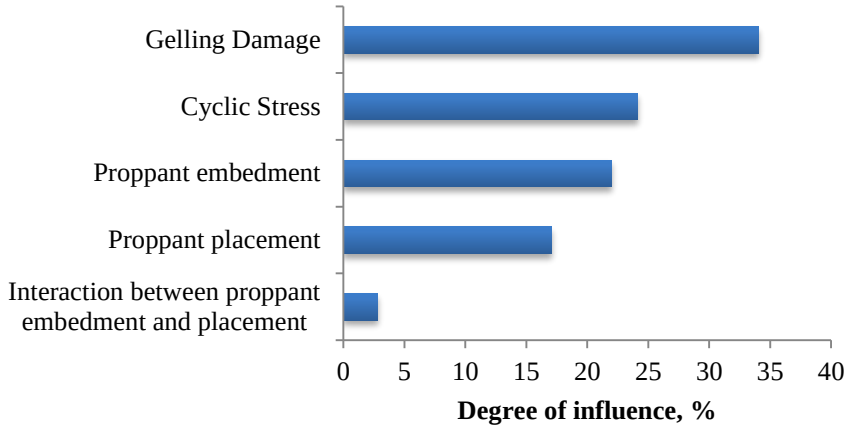

(a) Short-term (7 years)

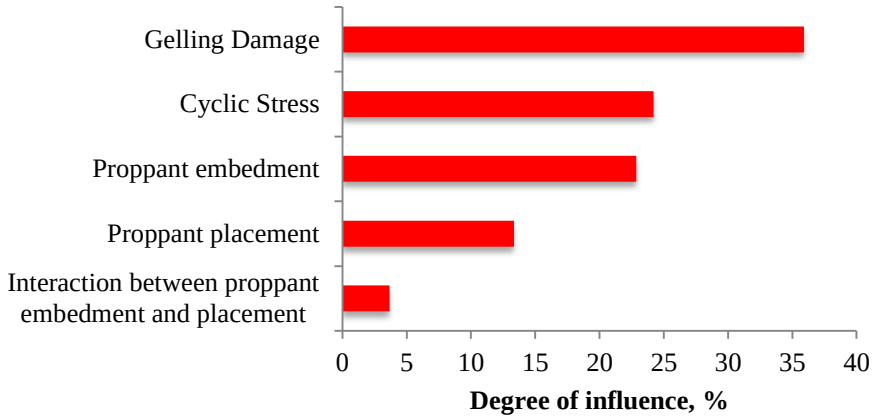

(b) Long-term (15 years)

Figure 56. Rank of critical parameters on well performance

On the other hand, reducing gel residue deposition as much as I can for intermediate or higher proppant concentration is ideal. It can be done by 1) using fracturing fluid with low polymer loading concentration, even though viscosity is expected to decrease (proppant placement and transport is not important). 2) Using high quality fracturing fluid and breaker such as residue free fracturing fluid. 3) allowing more time for breaking polymer chains.

4.3 Selection of Proppant

The choice of proppant is an important factor that dictates success of stimulation, especially for unconventional reservoirs with multistage hydraulic fracturing. In that case, tons of proppant are injected, and its cost composes a significant part of the total stimulation cost. The right proppant selection can maximize Net Present Value (NPV) for each well. However, with current low oil prices, and for the sake of more precise analysis, I introduced Profitability Ratio (PIR) to capture best proppant option due to different costs associated for each proppant. For example, proppant cost can be varied form 20 % for using natural sand to 50 % or more of total treatment cost when manufactured proppant is used (Brannon and Starks 2009). This is reason why PIR is more effective than NPV analysis.

$$NPV = \sum_{t=1}^{n} \frac{CF_t}{(1+i)^t} - (C_{D\&C} + C_{STIM}) \quad (15)$$

$$CF_t = (\text{yearly production rate x product price}) - \text{Royalties} - \text{Operating cost} - \text{income tax} \quad (16)$$

$$PIR = \frac{NPV}{Initial\ investment} = \frac{NPV}{(C_{D\&C} + C_{STIM})} \quad (17)$$

Where CF_t is after-tax project cash flow, $C_{D\&C}$ is drilling and completion cost, C_{STIM} is stimulation cost, i is interest rate, and t is number of years. Cost and revenue parameters are shown in **Table 8 and 9.** My assumption is that only single bi-wing fracture is modeled from 80 fractures within 5000 ft. of the lateral wellbore. Hence, the cost and revenue associated in this model are based on a single fracture. In proppant selection analysis, bi-wing hydraulic fracture is modeled with the half fracture length of 400 ft. and proppant concentration of each proppant is varied from low, intermediate, and high concentration.

Table 8. Cost associated in proppant selection analysis

Operation	Parameter	Cost
Drilling	Horizontal drilling, $/fracture	27812.5
Stimulation	Fixed cost, $	25000
	Pumping, $	9113.5
	Proppant handling and transport, $/lb	0.015
	Fracturing fluid, $/bbl	15
	Proppant, $/lb	
	Sand	0.0385
	Resin-coated Sand	0.22
	Ceramic	0.585
Others	Royalties, %	12.5
	Operation cost, $/bbl of oil	20
	Depreciation, year	7 (straight line)
	Income tax, %	35
	Interest rate, %	10

Table 9. Revenue associated in proppant selection analysis

Revenue	Value
Oil price, $/bbl	45
Gas price, $/Mscf	2.2

Also, damaging parameters are incorporated based on behavior of each proppant from laboratory observation as shown in **Table 10.** Proppant placement is uncertain, depending on stress heterogeneity as mentioned earlier, so both low and high convection scenarios are modeled. For gelling damage, we use the average minimum and maximum value from **Table 6**. Fine migration and plugging effect (**Figure 36**) show that permeability loss over 10 days is very high (99%) when sand is used as proppant while there is no permeability drop in the case of RCS due to its capability to capture fine. In this analysis, bottom hole pressure is set at 1500 psi to imitate real production conditions (largest choke strategy), so I expected to produce both oil and gas at the surface condition.

Table 10. Damaging parameter associated with each type of proppant

	Gelling damage	Proppant embedment	Proppant Placement	Cyclic stress	Fine migration and plugging
Sand	60 %	0.001 in	Both	20	99 %
RCS	60 %	0.000 in	Both	20	0 %
Ceramic	60 %	0.002 in	Both	20	70 %

Oil and gas cumulative production of the three proppants for low and intermediate proppant concentration over 15 years is shown in **Figure 57 and 58**. As a result, RCS performs better than sand and ceramic proppant in all ranges of proppant concentration for both low and high convection scenarios due to low proppant embedment and fine plugging, even though, ceramic proppant has a higher crushing resistance than RCS. However, as proppant concentration increased, cumulative production of ceramic proppant comes close to that of RCS proppant. The reason is the proppant embedment effect is less pronounced on well productivity as mentioned in the sensitivity study section.

On the other hand, selection of proppant by using only performance evaluation is not enough. Economic analysis must be done to examine cost effectiveness for each proppant by incorporating the economic parameters in **Table 8 and 9**. NPV and PIR for each proppant with all ranges of proppant concentration are shown in **Figure 59 and 60**. RCS is undoubtedly the most cost effective proppant for both low and high convection scenarios based on both NPV and PIR. Hence, RCS is the suitable proppant based on both performance and economics evaluation for this particular reservoir property. However, RCS has the temperature limit as defined by glass transition temperature (T_g); therefore, reservoir temperature is important factor for fracturing design with RCS as proppant. In

the next section, optimization of half fracture length and proppant concentration is studied with RCS as a proppant.

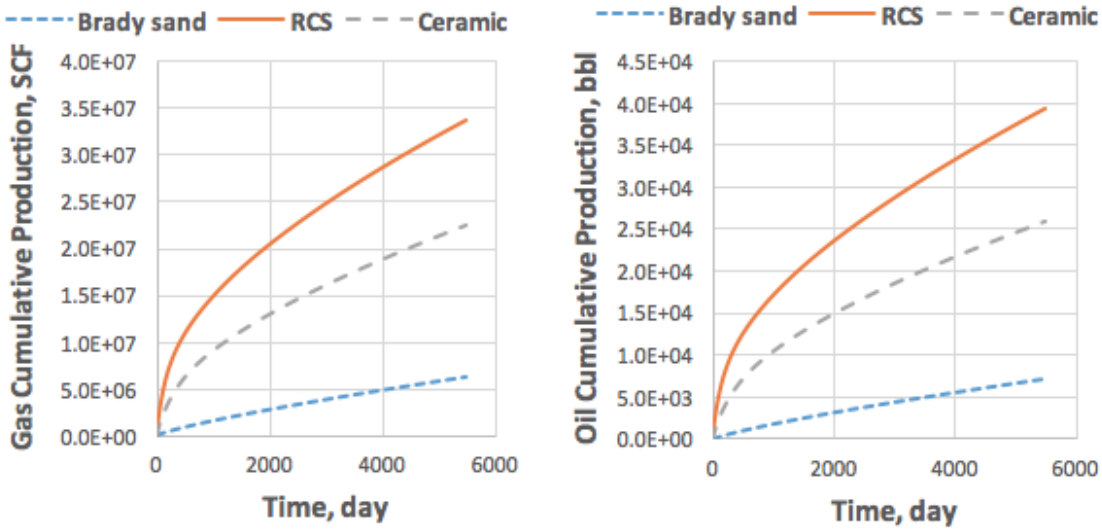

(a) Gas cumulative production (b) Oil cumulative production

Low convection effect

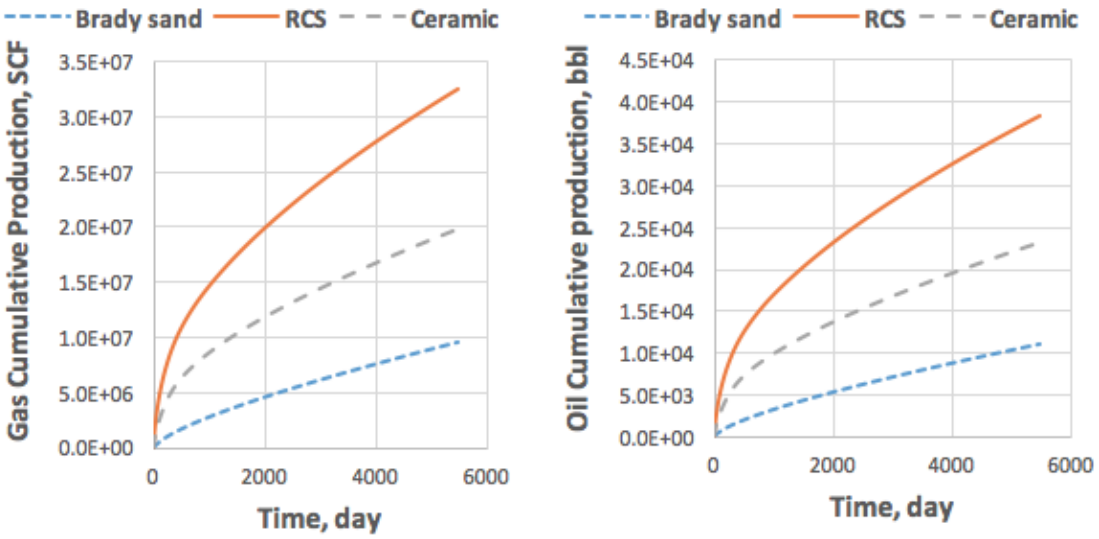

(c) Gas cumulative production (d) Oil cumulative production

High convection effect

Figure 57. Oil and gas cumulative production of three proppant type based on low proppant concentration (a), (b), (c), and (d)

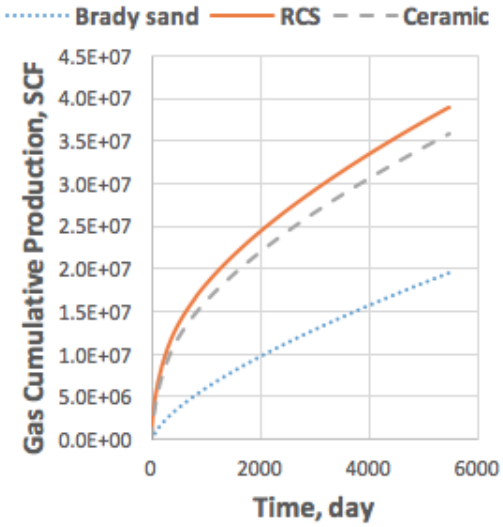

(a) Gas cumulative production

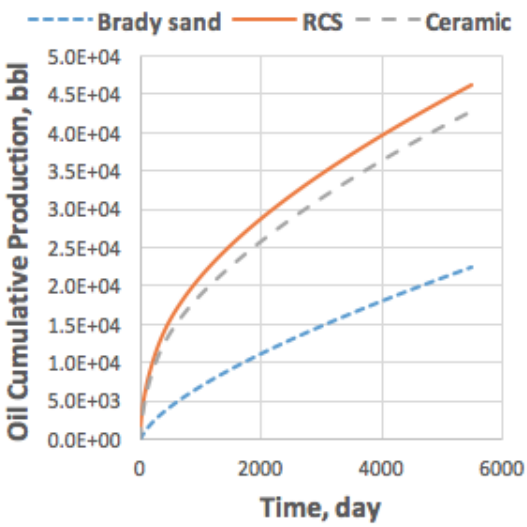

(b) Oil cumulative production

Low convection effect

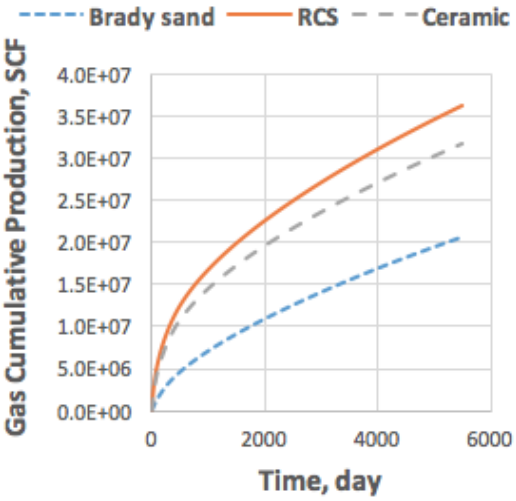

(c) Gas cumulative production

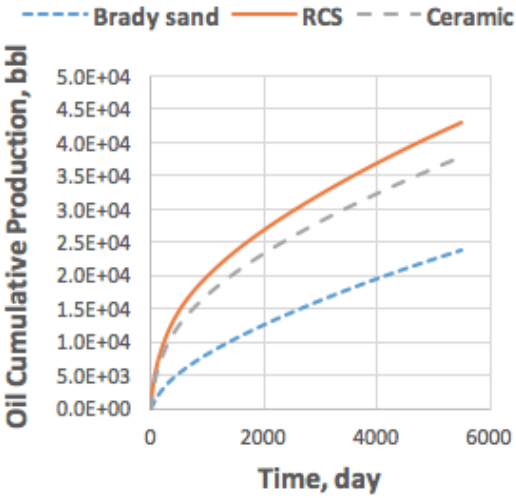

(d) Oil cumulative production

High convection effect

Figure 58. Oil and gas cumulative production of three proppant type based on intermediate proppant concentration (a), (b), (c), and (d)

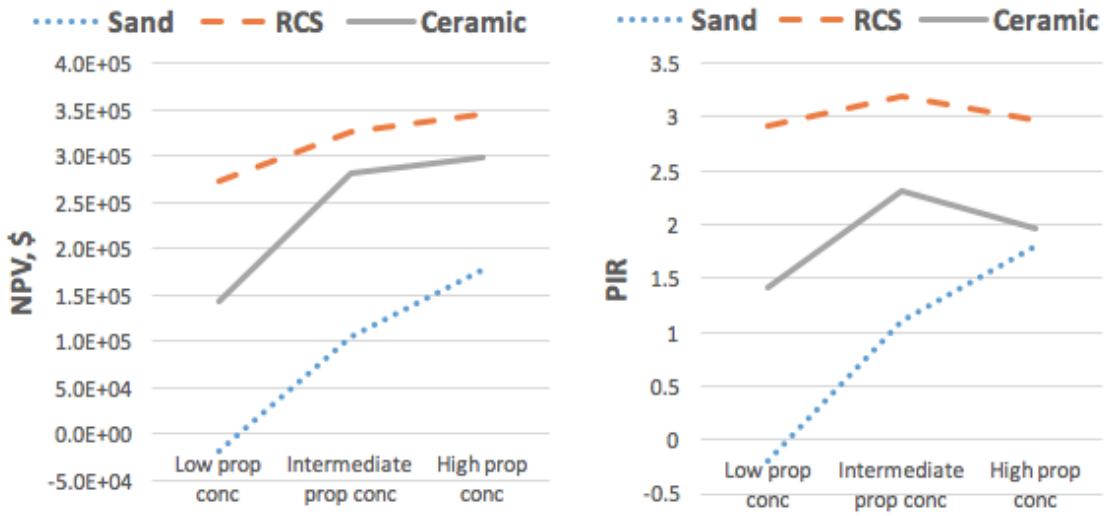

Figure 59. Net present value (NPV) and profitability ratio (PIR) of three type of proppant with low convection effect associated

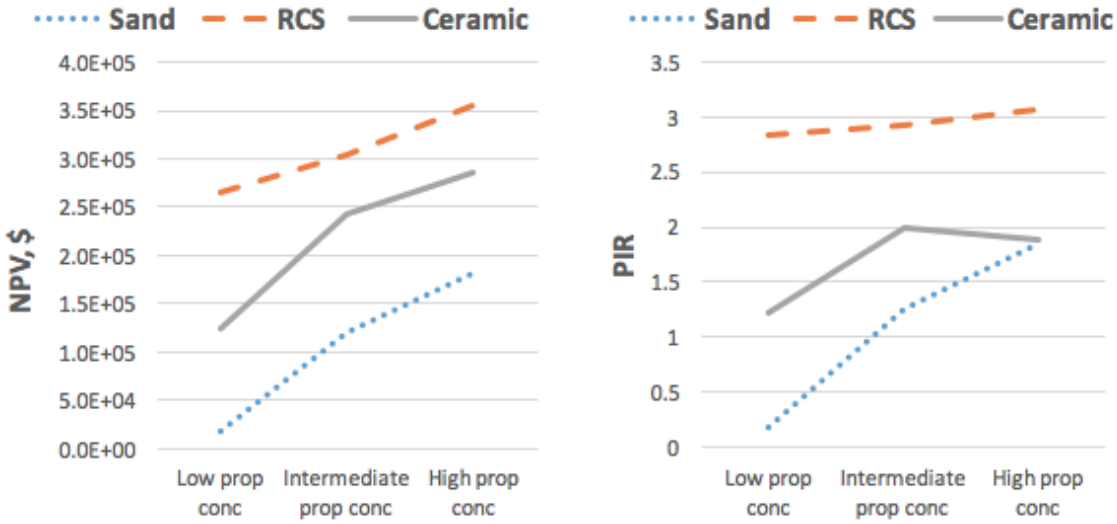

Figure 60. Net present value (NPV) and profitability ratio (PIR) of three types of proppant with high convection effect associated

Moreover, reducing fracturing (initial) cost while keeping the same well productivity is main goal during oil industry turmoil. The following example will show how proppant selection can fulfill this goal. **Figure 61** show oil cumulative production and initial cost for two different proppant type in many proppant concentration ranges. This example is a comparison between the cases of RCS at low proppant concentration

and sand with high proppant concentration. For RCS, oil cumulative production is 39,436 bbl and initial cost is $93,927 while oil cumulative production and initial cost are 30,278 bbl and $98,266 for case of sand respectively. Hence, Using RCS instead of sand for stimulation design can decrease initial cost by 4.4 % but significantly increase oil cumulative production by 30.3 % as shown in **Appendix A1**. This example show that selection of proppant is very important in hydraulic fracturing design because different proppant types have varied conductivity damaging parameter associated and cost.

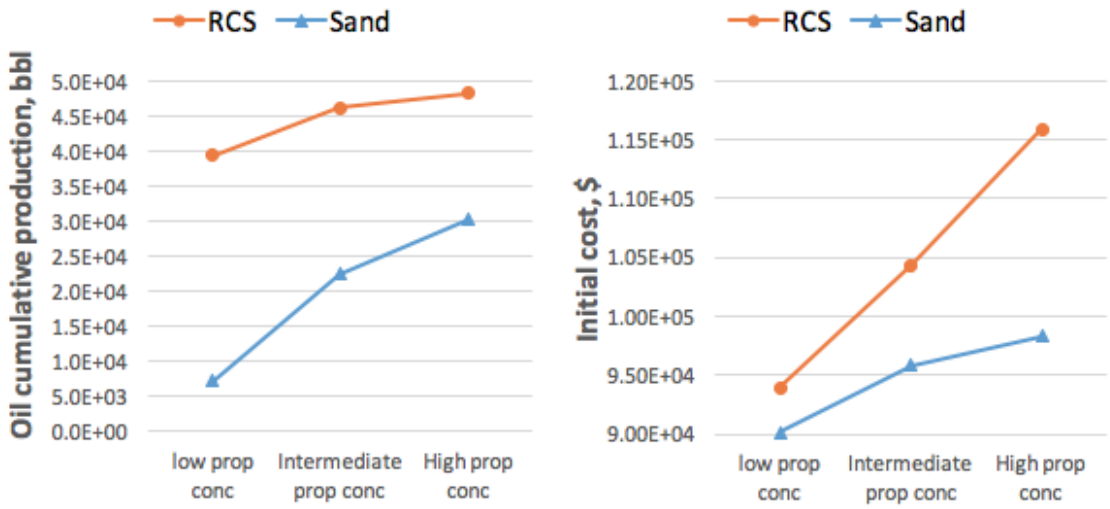

Figure 61. Oil cumulative production over 15 years and initial cost for different proppant type

4.4 Optimization of Fracture Design

The cost of hydraulic fracturing is tremendous, so optimal fracture half-length and proppant concentration must be investigated. As I increase the fracture half-length with the same fracture width, a higher amount of fracturing fluid and proppant are needed. Moreover, the amount of proppant required is enlarged if I increase fracture width. Therefore, both escalating fracture length and proppant concentration can inflate associated hydraulic fracturing cost, even though well productivity is enhanced (Liang et

al. 2015). This is the reason why I introduce PIR to capture and compare between increasing well productivity (profit) and cost. In this model, the fracture half-length and average proppant concentration are varied from 200-500 ft. and 0.04-0.46 lb/ft^2, respectively. The proppant type is RCS with low convection effect.

First, optimal half-fracture length is investigated. The cumulative oil production of each fracture half-length throughout all ranges of average proppant concentration is shown in **Figure 62**, illustrating that the longer half fracture length results in significantly higher cumulative oil production while increasing fracture width gradually increases cumulative oil production. Hence, fracture length is more important for well productivity than fracture width in this scenario. The economic analysis is investigated based on NPV and PIR as shown in **Figure 63.** Based on NPV analysis, a fracture with 500 ft. half-length possesses highest NPV for all ranges of proppant concentration. On the other hand, a fracture with 400 ft. half-length has highest PIR. From optimization criteria based on current low oil prices, reducing fracturing cost while maintaining well performance are important issues, so PIR analysis might be a more useful tool when compared with NPV analysis. Hence, the optimal fracture half-length is 400 ft.

The following example will show how PIR can satisfy industry goal (reducing cost while remaining the well productivity). **Figure 64** illustrates the oil cumulative production and initial cost of 400 and 500 ft. fracture half-length with different proppant concentrations. This example will compare the cases of 400 ft. half-length with 0.24 average proppant concentration and 500 ft. half-length with 0.04 average proppant concentration. Both case have almost the same oil cumulative production but initial cost

of the former and later case are $116,644 and $121,165 respectively. Therefore, using PIR for fracturing design can decrease initial cost by 3.7 % as shown in **Appendix A2**.

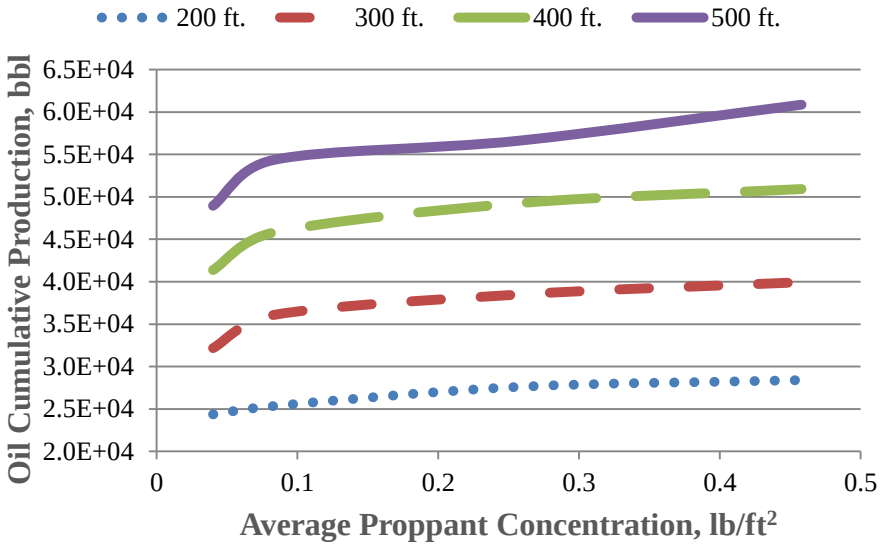

Figure 62. Oil cumulative production with different fracture half-length (Xf)

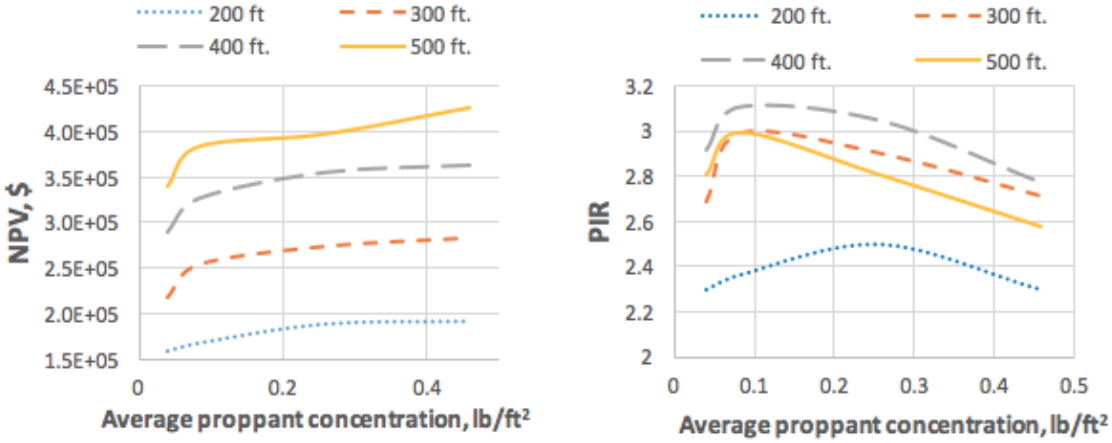

Net present value (NPV) Profitability ratio (PIR)

Figure 63. NPV and PIR with different fracture half-length (Xf)

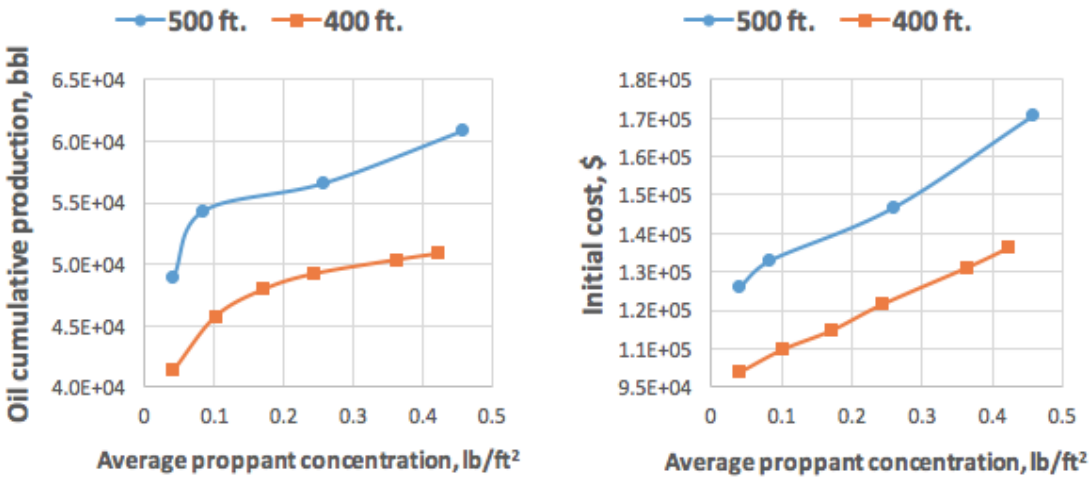

Figure 64. Oil cumulative production over 15 years and initial cost for different fracture half-length

Finally, optimal proppant concentration and conductivities are examined as shown in **Figure 65,** illustrating that increasing proppant concentration from 0.04-0.24 lb/ft^2 can sharply increase NPV, while further increasing proppant concentration does not have much effect on NPV. The reason is the degree of increasing cost associated overcoming productivity enhancement. Hence, the optimal average proppant concentration and conductivities based on PIR are 0.17 lb/ft^2 and 50 mD-ft respectively. In this case, using PIR instead of NPV, I can reduce the initial cost by at least 16 %, while reduction of NPV is less than 5 %, as shown in **Figure 66 and Appendix A3**. Instead of using at least $131,000 based on NPV, the Initial cost is $110,000 based on PIR, so I can save $21000 per fracture. Therefore, reduction of initial cost associated with 80 stage fracture is at least $1,680,000.

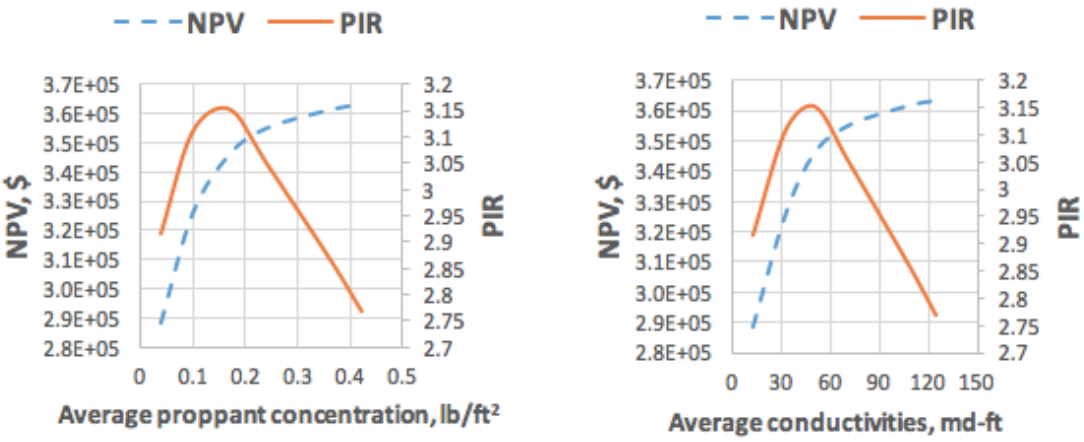

Based on proppant concentration Based on fracture conductivities

Figure 65. NPV and PIR with different fracture width

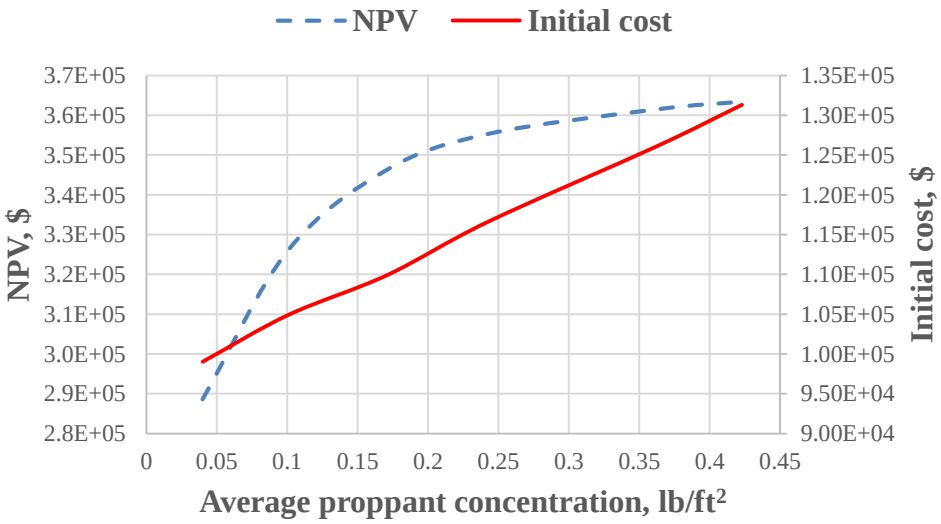

Figure 66. NPV and initial cost with different fracture width

Conclusions

The unfavorable effects of gelling damage, proppant indentation, proppant placement, cyclic stress, and fine plugging on well productivity are studied. Sensitivity analysis is performed to quantify the most important parameters for low and intermediate proppant concentrations. I also examined the selection of proppant based on profitability ratio (PIR) and net present value (NPV) approach. Finally, optimal half fracture length, average proppant concentration, and conductivities are investigated. The following conclusions can be drawn:

(1) Combination of damaging effects can significantly reduce the well performance and thus should be considered for fracturing design. However, the productivity decline varies depending upon many factors, such as reservoir properties and heterogeneities, proppant type, or proppant concentration.

(2) Proppant embedment and placement are very significant damaging factors in low proppant concentration environment (narrow width fractures). However, their importance diminishes in intermediate proppant concentration.

(3) Resin coated sand (RCS) seems quite promising from both performance and economic perspectives for cases studied here; because it illustrates low proppant embedment and the ability to capture generated fine particle. However, the properties of resin are expected to change at different temperature especially when reservoir temperature is above glass transition temperature (T_g); therefore, using RCS should be selected based on reservoir temperature.

(4) The optimal fracture half-length, average proppant concentration, and fracture conductivity are 400 ft, 0.17 lb/ft^2, and 50 mD-ft, respectively for particular reservoir property in this study.

(5) Profitability ratio (PIR) is a good economic measure for hydraulic fracturing design that can reduce the estimated initial cost at least 16 % for cases studied in this thesis.

Future Work

Some assumptions are made in this work due to simplicity of modelling and lack of experimental data. To duplicate real fracture conditions, additional laboratory-base measurement or fracture modelling is needed. Below is an example of future research topics that can improve our simulation model.

1. Permeability or conductivity decline as a function of stress due to crushing of proppant at different proppant concentration rather than 2 lb/ft^2.
2. Modelling of rough fracture face and proppant displacement inside fracture (**Figure 44**) by using specific software such as COMSOL. Those models should be able to determine the effect of arches, pillars, and void space on fracture conductivity.
3. The relationship between each of conductivity damaging parameters is crucial to determine the combined effect.
4. Reservoir properties such as natural fracture is needed to incorporate into both hydraulic fracturing and reservoir model. Also, with association of microseismic analysis, simulated reservoir volume (SRV) can be determined. Hence, fracture network can be modeled.

References

Abass, H. H., Al-Tahini, A. M., Abousleiman, Y., and Khan, M. R. 2009. New Technique to Determine Biot Coefficient for Stress-Sensitive Dual-Porosity Reservoirs. Presented at the SPE Annual Technical Conference and Exhibition, New Orleans, Louisiana, 4-7 October. SPE-124484-MS. http://dx.doi.org/10.2118/124484-MS

Aggour, T. M., and Economides, M. J. 1996. Impact of fluid selection on high-permeability fracturing. Presented at European Petroleum Conference, Milan, Italy, 22-24 October. SPE-36902-MS. http://dx.doi.org/10.2118/36902-MS

Alramahi, B., and Sundberg, M. 2012. Proppant embedment and conductivity of hydraulic fractures in shales. Presented at the 46th US Rock Mechanics/Geomechanics Symposium, Chicago, Illinois, 24-27 June. ARMA-2012-291.

API RP 61, Recommended Practices for Evaluating Short Term Proppant Pack Conductivity. 1989. Washington, DC: API.

Barree, R., and Conway, M. 1994. Experimental and numerical modeling of convective proppant transport. Presented at the SPE Annual Technical Conference and Exhibition, New Orleans, Louisiana, 25-28 September. SPE-28564-MS. http://dx.doi.org/10.2118/28564-MS.

Bazan, L. W., Larkin, S. D., Lattibeaudiere, M. G., and Palisch, T. T. 2010. Improving production in the Eagle Ford shale with fracture modeling, increased fracture conductivity, and optimized stage and cluster spacing along the horizontal wellbore. Presented at the Tight Gas Completions Conference, San Antonio, Texas, 2-3 November. SPE-138425-MS. http://dx.doi.org/10.2118/138425-MS.

Brannon, H. D., and Starks, T. R. 2009. Maximizing Return-On-Fracturing-Investment by Using Ultra-Lightweight Proppants to Optimize Effective Fracture Area: Can Less Be More? Presented at the SPE Hydraulic Fracturing Technology Conference, The Woodlands, Texas, 19-21 January. SPE-119385-MS. http://dx.doi.org/10.2118/119385-MS.

Cipolla, C. L., Warpinski, N. R., Mayerhofer, M. J., Lolon, E., and Vincent, M. C. 2008. The relationship between fracture complexity, reservoir properties, and fracture treatment design. Presented at the SPE Annual Technical Conference and Exhibition, Denver, Colorado, 21-24 September. SPE-115769-MS. http://dx.doi.org/10.2118/115769-MS.

Clark, P. E., Harkin, M. W., Wahl, H. A., and Sievert, J. A. 1977. Design of a large vertical prop transport model. Presented at the SPE Annual Fall Technical Conference and Exhibition, Denver, Colorado, 9-12 October. SPE-6814-MS. http://dx.doi.org/10.2118/6814-MS.

Clark, P. E. 2006. Transport of proppant in hydraulic fractures. Presented at the SPE Annual Technical Conference and Exhibition, San Antonio, Texas, 24-27 September. SPE-103167-MS. http://dx.doi.org/10.2118/103167-MS.

Cleary, M. P., and Fonseca Jr, A. 1992. January. Proppant convection and encapsulation in hydraulic fracturing: practical implications of computer and laboratory simulations. Presented at the SPE Annual Technical Conference and Exhibition, Washington, D.C., 4-7 October. SPE-24825-MS. http://dx.doi.org/10.2118/24825-MS.

Collins, P., Badessich, M. F., and Ilk, D. 2015. Addressing Forecasting Non-Uniqueness and Uncertainty in Unconventional Reservoir Systems Using Experimental Design. Presented at the SPE Annual Technical Conference and Exhibition, Houston, Texas, 28-30 September. SPE-175139-MS. http://dx.doi.org/10.2118/175139-MS.

Cooke Jr, C. 1975. Effect of fracturing fluids on fracture conductivity. J Pet Technol 27 (10): 1,273-271,282. SPE-5114-PA. http://dx.doi.org/10.2118/5114-PA.

Denney, D. 2012. Fracturing-Fluid Effects on Shale and Proppant Embedment. . J Pet Technol 64 (03): 59-61. SPE-0312-0059-JPT. http://dx.doi.org/10.2118/0312-0059-JPT.

Dewprashad, B., Abass, H. H., Meadows, D. L., Weaver, J. D., and Bennett, B. J. 1993. A method to select resin-coated proppants. Presented at the SPE Annual Technical Conference and Exhibition, Houston, Texas, 3-6 October. SPE-26523-MS. http://dx.doi.org/10.2118/26523-MS.

Economides, M. J., and Wang, X. 2010. Design flaws in hydraulic fracturing. Presented at the SPE International Symposium and Exhibiton on Formation Damage Control, Lafayette, Louisiana, 10-12 February. SPE-127870-MS. http://dx.doi.org/10.2118/127870-MS.

Geertsma, J., and De Klerk, F. 1969. A rapid method of predicting width and extent of hydraulically induced fractures. J Pet Technol 21 (12): 1-571. SPE-2458-PA. http://dx.doi.org/10.2118/2458-PA.

Ghosh, S., Rai, C. S., Sondergeld, C. H., and Larese, R. E. 2014. Experimental Investigation of Proppant Diagenesis. Presented at the SPE/CSUR Unconventional Resources Conference–Canada, Calgary, Alberta, 30 September–2 October. SPE-171604-MS. http://dx.doi.org/10.2118/171604-MS.

Gidley, J., Penny, G., and McDaniel, R. 1995. Effect of proppant failure and fines migration on conductivity of propped fractures. SPE Prod & Fac 10 (01): 20-25. SPE-24008-PA. http://dx.doi.org/10.2118/24008-PA.

Han, J., and Wang, J. Y. 2014. Fracture Conductivity Decrease Due to Proppant Deformation and Crushing, a Parametrical Study. Presented at the SPE Eastern Regional Meeting, Charleston, WV, 21-23 October. SPE-171019-MS. http://dx.doi.org/10.2118/171019-MS.

Han, J., Yang, J., Sookprasong, A., and Lafollette, R. 2015. Numerical Study of Fracture Cleanup Effects and Optimization of Post-Fracture Production. Presented at the SPE European Formation Damage Conference and Exhibition, Budapest, Hungary, 3-5 June. SPE-174201-MS. http://dx.doi.org/10.2118/174201-MS.

Hyne, N. 2014. Dictionary of petroleum exploration, drilling & production. PennWell Corporation.

ISO13503-2:2006/Amd.1:2009(E): 2006, Petroleum and Natural Gas Industries-Completion Fluids and Materials- Part 5: Procedures for Measuring the Long-Term Conductivity, First Edition. 2006. Geneva, Switzerland: ISO.

Liang, F., Sayed, M., Al-Muntasheri, G., and Chang, F. F. 2015. Overview of Existing Proppant Technologies and Challenges. Presented at the SPE Middle East Oil & Gas Show and Conference, Manama, Bahrain, 8-11 March. SPE-172763-MS. http://dx.doi.org/10.2118/172763-MS.

Mack, M., Sun, J., and Khadilkar, C. 2014. Quantifying Proppant Transport in Thin Fluids: Theory and Experiments. Presented at the SPE Hydraulic Fracturing Technology Conference, The Woodlands, Texas, 4-6 February. SPE-168637-MS. http://dx.doi.org/10.2118/168637-MS.

Manrique, J. F., and Poe, B. D. 2007. Evaluation and optimization of low conductivity fractures. Presented at the SPE Hydraulic Fracturing Technology Conference, College Station, Texas, 29-31 January. SPE-106317-MS. http://dx.doi.org/10.2118/106317-MS.

Mata, D., Cherian, B., and Gonzales, V. 2014. Modeling the Influence of Pressure Depletion in Fracture Propagation and Quantifying the Impact of Asymmetric Fracture Wings in Ultimate Recovery, Presented at the SPE Unconventional Resources Conference, Woodlands, Texas, 1–3 April 2014. SPE-169003-MS. http://dx.doi.org/10.2118/169003-MS.

Montgomery, C. T., and Smith, M. B. 2010. Hydraulic fracturing: history of an enduring technology. J Pet Technol 62 (12): 26-40. SPE-1210-0026-JPT. http://dx.doi.org/10.2118/1210-0026-JPT.

Ouabdesselam, M., and Hudson, P. 1991. An Investigation of the Effect of Cyclic Loading on Fracture Conductivity. Presented at the SPE Annual Technical Conference and Exhibition, Dallas, Texas, 6-9 October. SPE-22850-MS. http://dx.doi.org/10.2118/22850-MS.

Outlook, A. E. 2013. US Energy Information Administration Washington: DC

Palisch, T. T., Duenckel, R. J., Chapman, M. A., Woolfolk, S., and Vincent, M. C. 2009. How to Use and Misuse Proppant Crush Tests--Exposing the Top 10 Myths. Presented at the SPE Hydraulic Fracturing Technology Conference, The Woodlands, Texas, 19-21 January.SPE-119242-MS. http://dx.doi.org/10.2118/119242-MS.

Palisch, T. T., Vincent, M., and Handren, P. J. 2010. Slickwater fracturing: food for thought. SPE Prod & Oper 25 (03): 327-344. SPE-115766-PA. http://dx.doi.org/10.2118/115766-PA.

Perkins, T. K., and Kern, L. R. 1961. Widths of hydraulic fractures. J Pet Technol 13 (09): 937-949. SPE-89-PA. http://dx.doi.org/10.2118/89-PA.

Quintero, J., and Devegowda, D. 2015. Modelling Based Recommendation for Choke Management in Shale Wells. Presented at the Unconventional Resources Technology Conference, San Antonio, Texas, 20-22 July. SPE-178639-MS. http://dx.doi.org/10.2118/178639-MS.

Romero, D. J., Valko, P. P., and Economides, M. J. 2002. The Optimization Of The Productivity Index And The Fracture Geometry Of A Stimulated Well With Fracture Face And Choke Skins. Presented at the International Symposium and Exhibition on Formation Damage Control, Lafayette, Louisiana, 20-21 February. SPE-73758-MS. http://dx.doi.org/10.2118/73758-MS.

Rubin, B. 2010. Accurate simulation of non Darcy flow in stimulated fractured shale reservoirs. Presented at the SPE Western Regional Meeting, Anaheim, California, 27-29 May. SPE-132093-MS. http://dx.doi.org/10.2118/132093-MS.

Sahai, V., Jackson, G., and Rai, R. R. 2013. Effect of Non-uniform Fracture Spacing and Fracture Half-length on Well Spacing for Unconventional Gas Reservoirs. Presented at the EAGE Annual Conference & Exhibition incorporating SPE Europec, London, UK, 10-13 June. SPE-164927-MS. http://dx.doi.org/10.2118/164927-MS.

Saldungaray, P. M., and Palisch, T. T. 2012. Hydraulic fracture optimization in unconventional reservoirs. Presented at the SPE Middle East Unconventional Gas Conference and Exhibition, Abu Dhabi, UAE, 23-25 January. SPE-151128-MS. http://dx.doi.org/10.2118/151128-MS.

Saucier, R. J. 1974. Considerations in gravel pack design. J Pet Technol 26 (02): 205-212. SPE-4030-PA. http://dx.doi.org/10.2118/4030-PA.

Schubarth, S., and Milton-Tayler, D. 2004. Investigating how proppant packs change under stress. Presented at the SPE Annual Technical Conference and Exhibition, Houston, Texas, 26-29 September. SPE-90562-MS. http://dx.doi.org/10.2118/90562-MS.

Shah, S. N., and Asadi, M. 1998. Convection/Encapsulation in Hydraulic Fracturing. Presented at the SPE Rocky Mountain Regional/Low-Permeability Reservoirs Symposium, Denver, Colorado, 5-8 April. SPE-39961-MS. http://dx.doi.org/10.2118/39961-MS.

Shah, S. N., Vincent, M. C., Rodriquez, R. X., and Palisch, T. T. 2010. Fracture orientation and proppant selection for optimizing production in horizontal wells. Presented at the SPE Oil and Gas India Conference and Exhibition, Mumbai, India, 20-22 January. SPE-128612-MS. http://dx.doi.org/10.2118/128612-MS.

Stephens, W. T., Schubarth, S. K., Dickson, K. R., Snyder, E. M., Doles, K., and Herndon, D. C. 2007. Behavior of proppants under cyclic stress. Presented at the SPE Hydraulic Fracturing Technology Conference, College Station, Texas, 29-31 January. SPE-106365-MS. http://dx.doi.org/10.2118/106365-MS.

Suarez-Rivera, R., Burghardt, J., Edelman, E., Stanchits, S., and Surdi, A. 2013. Geomechanics considerations for hydraulic fracture productivity. Presented at the 47th US Rock Mechanics/Geomechanics Symposium, San Francisco, California, 23-26 June. ARMA-2013-666.

Vincent, M. C. 2009. Examining Our Assumptions--Have Oversimplifications Jeopardized Our Ability to Design Optimal Fracture Treatments? Presented at the SPE Hydraulic Fracturing Technology Conference, The Woodlands, Texas, 19-21 January. SPE-119143-MS. http://dx.doi.org/10.2118/119143-MS.

Warpinski, N. 2014. A review of hydraulic-fracture induced microseismicity. Presented at the 48th US Rock Mechanics/Geomechanics Symposium, Minneapolis, Minnesota, 1-4 June. ARMA-2014-777.

Weaver, J. D., Nguyen, P. D., Parker, M. A., and van Batenburg, D. W. 2005. Sustaining fracture conductivity. Presented at the SPE European Formation Damage Conference, Sheveningen, The Netherlands, 25-27 May. SPE-94666-MS. http://dx.doi.org/10.2118/94666-MS.

Weaver, J. D., Parker, M., van Batenburg, D. W., and Nguyen, P. D. 2007. Fracture-Related Diagenesis May Impact Conductivity. SPE J 12 (03): 272-281. SPE-98236-PA. http://dx.doi.org/10.2118/98236-PA.

Weaver, J. D., Rickman, R. D., Luo, H., and Logrhy, R. 2009. A Study of Proppant Formation Reactions. Presented at the SPE International Symposium on Oilfield Chemistry, The Woodlands. Texas, 20-22 April. SPE-121465-MS. http://dx.doi.org/10.2118/121465-MS.

Weaver, J., Liang, F., and Schultheiss, N. 2015. Assessment of Fracturing-Fluid Cleanup by Use of a Rapid-Gel-Damage Method. SPE Prod & Oper 30 (01): 69-75. SPE-165086-PA. http://dx.doi.org/10.2118/165086-PA

Xiong, Y., Winterfeld, P., Wang, C., Huang, Z., and Wu, Y.-S. 2015. Effect of Large Capillary Pressure on Fluid Flow and Transport in Stress-sensitive Tight Oil Reservoirs. Presented at the SPE Annual Technical Conference and Exhibition, Houston, Texas, 28-30 September. SPE-175074-MS. http://dx.doi.org/10.2118/175074-MS.

Yang, M., Economides, M. J., Wei, C., and Gao, C. 2013. Hydraulic Fracture Design Flaws-Proppant Selection. Presented at the SPE Annual Technical Conference and Exhibition, New Orleans, Louisiana, 30 September-2 October. SPE-166299-MS. http://dx.doi.org/10.2118/166299-MS.

Yang, Y., Robart, C. J., and Ruegamer, M. 2013. Analysis of US hydraulic fracturing fluid system trends. Presented at the SPE Hydraulic Fracturing Technology Conference, The Woodlands, Texas, 4-6 February. SPE-163875-MS. http://dx.doi.org/10.2118/163875-MS.

Yasuhara, H., Elsworth, D., and Polak, A. 2003. A mechanistic model for compaction of granular aggregates moderated by pressure solution. Journal of Geophysical Research: Solid Earth, 108 (B11).

Zhang, J., Zhu, D., and Hill, A. D. 2015. A new theoretical method to calculate shale fracture conductivity based on the population balance equation. Journal of Petroleum Science and Engineering, 134, 40-48.

Appendix A: Calculations

A1

% initial cost reduction = $\frac{98{,}266-93{,}927}{98{,}266} * 100$ = 4.41 %

% oil cumulative increased = $\frac{39{,}436-30{,}278}{30{,}278} * 100$ = 30.25 %

A2

% initial cost reduction = $\frac{121165-116644}{121165} * 100$ = 3.73%

A3

% initial cost reduction = $\frac{131{,}321-109{,}907}{131{,}321} * 100$ = 16.31 %

% NPV reduction = $\frac{363{,}439-346{,}316}{363{,}439} * 100$ = 4.71 %

Initial cost reduction per fracture = $131321 - 109907$ = $21,414

Initial cost reduction for multistage fracture (80) = $21{,}414 * 80$ = $1,713,120

Appendix B: Experiment Descriptions and Conditions

B1

Ghosh et al. (2014) measures permeability loss in the proppant pack with time (10 days) for three different types of proppant. The experimental condition and set-up are shown in the table below for test 9-12.

Table 11. Experiment condition and set-up (Ghosh et al. 2014)

Parameters	
Type of core(Formation)	1 inch diameter Barnett Shale core plugs (Clay and quartz rich)
Pore pressure	1000 psi
Confining pressure	5000 psi
Temperature	225 °F
Fluid	Brine
Fluid flow rate	3 ml/min

B2

Schubarth and Milon-Tayler (2004) investigate the effect of cyclic stress on proppant pack permeability by measuring median particle diameter changes for two types of proppant: sand and intermediate density ceramic. API crush test procedure (2 lb/ft^2 proppant concentration) was adopt to perform the test. The experiment condition and set-up are shown in the table below.

Table 12. Experiment condition and set-up (Schubarth and Milon-Tayler 2004)

Parameters	
Range of stress	2000-12000 psi
Loading stress rate	1000 psi per minute
Relieved stress rate	No more than 1000 psi per minute
Number of cyclic stress	5 and 20 cycles
Stress holding period	5 minutes